SENSITIVE AND QUANTITATIVE DETERMINATION OF CYSTEINE BY SURFACE ENHANCED RAMAN SPECTROMETRY BASED ON THEIR INDUCED AGGREGATES OF GOLD AND SILVER NANOSTRUCTURES

A THESIS SUBMITTED TO

THE GRADUATE SCHOOL OF NATURAL AND APPLIED SCIENCES

OF

MIDDLE EAST TECHNICAL UNIVERSITY

BY

RECEP YÜKSEL

IN PARTIAL FULFILLMENT OF THE REQUIREMENTS

FOR

THE DEGREE OF MASTER OF SCIENCE

IN

CHEMISTRY

SEPTEMBER 2011

Approval of the thesis;

SENSITIVE AND QUANTITATIVE DETERMINATION OF CYSTEINE BY SURFACE ENHANCED RAMAN SPECTROMETRY BASED ON THEIR INDUCED AGGREGATES OF GOLD AND SILVER NANOSTRUCTURES

submitted by **RECEP YÜKSEL** in a partial fulfillment of the requirements for the degree of **Master of Science in Chemistry Department, Middle East Technical University** by

Prof. Dr. Canan ÖZGEN
Dean, Graduate School of **Natural and Applied Sciences** _____

Prof. Dr. İlker ÖZKAN
Head of Department, **Chemistry** _____

Prof. Dr. Mürvet VOLKAN
Supervisor, **Chemistry Department, METU** _____

Examining Committee Members:

Prof. Dr. O. Yavuz ATAMAN
Department of Chemistry, METU _____

Prof. Dr. Mürvet VOLKAN
Department of Chemistry, METU _____

Prof. Dr. Semra KOCABIYIK
Department of Biology, METU _____

Prof. Dr. Ceyhan KAYRAN
Department of Chemistry, METU _____

Prof Dr. Necati ÖZKAN
Department of Polymer Science and Techn, METU _____

Date: 23.09.2011

I hereby declare that all information in this document has been obtained and presented in accordance with academic rules and ethical conduct. I also declare that, as required by these rules and conduct, I have fully cited and referenced all material and results that are not original to this work.

Name, Last name: Recep YÜKSEL

Signature

ABSTRACT

SENSITIVE AND QUANTITATIVE DETERMINATION OF CYSTEINE BY SURFACE ENHANCED RAMAN SPECTROMETRY BASED ON THEIR INDUCED AGGREGATES OF GOLD AND SILVER NANOSTRUCTURES

Yüksel, Recep

M.Sc., Department of Chemistry
Supervisor: Prof. Dr. Mürvet Volkan

September 2011, 76 pages

The synthesis of noble metal nanostructures are an active research area and controlling the shape and the size is a challenging task. In this study, nanostructures with different morphologies were prepared using wet chemical synthesis techniques in the aqueous solutions. Gold and silver nanospheres were produced by reducing and capping agent trisodium citrate. Gold nanorods were synthesized by chemical reduction of $HAuCl_4$ by ascorbic acid in the presence of cetyltrimethylammonium bromide (CTAB), $AgNO_3$, and gold nanoseeds (in 1.5 nm diameter) and gold silver core shell nanorods were prepared by addition of silver atoms on the surface of gold nanorods in the presence of CTAB. Parameters that were critical to obtain homogeneous nanostructures were optimized. The characterization of the nanoparticles was performed by UV-VIS spectrometry, High Resolution - Transition Electron Microscopy (HR-TEM), Field Emission - Scanning Electron Microscopy (FE-SEM) and Energy Dispersive X-ray Spectroscopy (EDX). Besides, their electromagnetic enhancement properties were demonstrated through SERS measurement of cysteine.

Self-assembly or assisted assembly of nanorods or nanospheres into organized arrays allows the realization of their collective properties that arise from the coupling of the optical and electronic properties of the neighbouring individual nanoparticles. In this study cysteine molecule was used as a linker molecule. The controlled addition of cysteine into the gold nanorod solution resulted in their preferential binding to the two ends of the gold nanorods and the formation of gold nanochains. In the usage of gold nanospheres on the other hand, cooperative hydrogen bonding of the cysteine molecules, resulted in the formation of gold nanoclusters. The assembly formation was demonstrated by UV–vis spectrometry and FE-SEM.

Cysteine is a thiol group containing amino acid and deficiency of cysteine results in serious health problems. Therefore, determination of cysteine is an important issue. Herein we report two strategies for the quantitative determination of micromolar concentrations of cysteine by exploiting the interplasmon coupling in Au nanoparticles. One of them is a recently published colorimetric method and the other is a novel SERS method.

Keywords: Cysteine, Gold, Silver, Nanoparticle, Nanorods, SERS

ÖZ

ALTIN VE GÜMÜŞ NANOYAPI KÜMELERİNE DAYANAN YÜZEYDE GÜÇLENDİRİLMİŞ RAMAN SPEKTROMETRİSİ İLE HASSAS VE KUANTİTATİF SİSTEİN TAYİNİ

Yüksel, Recep

Yüksek Lisans, Kimya Bölümü
Tez Yöneticisi: Prof. Dr. Mürvet Volkan

Eylül 2011, 76 sayfa

Soy metal nanoyapılarının sentezlenmesi aktif bir araştırma alanıdır ve nanoyapıların şekil ve boyutlarının kontrol edilmesi zor bir konudur. Bu çalışmada, farklı morfolojilerdeki nanoyapılar su ortamında yaş kimya sentez teknikleri kullanılarak hazırlandı. Altın ve gümüş nanoküreler, indirgeyici ve stabilize edici madde trisodyum sitrat ile hazırlandı. Altın nanoçubuklar, askorbik asit, sürfaktant setiltrimetilamonyum bromür (CTAB)'ın , gümüş nitrat ve altın nanoçekirdekler (1.5 nm çap) sayesinde $HAuCl_4$'ün kimyasal indirgenmesiyle sentezlendi. Altın gümüş öz kabuk nanoçubuklar ise CTAB ortamında gümüş atomlarının altın nanoçubukların üzerine eklenmesiyle üretildi. Homojen nanoparçacıklar üretilmesi için gereken parametreler optimize edildi. Nanoparçacıkların karakterizasyonu UV-VIS spektrometri, Yüksek Çözünürlük- Geçirimli Elektron Mikroskopi, Alan Emisyonlu – Taramalı Elektron Mikroskopi ve Enerji Dağılımlı X- Işını Spektroskopi teknikleriyle yapıldı. Bunun yanı sıra nanoyapıların elektromanyetik güçlendirme

özellikleri Sistein'in Yüzeyde Güçlendirilmiş Raman Saçılımı (YGRS) ölçümleri ile gösterildi.

Düzenlenmiş sıralardaki kendiliğinden dizilen ya da yardım ile dizilen nanoçubuklar ya da nanoküreler komşu yalnız nanoparçacıkların optik ve elektronik özelliklerinin örtüşmesiyle meydana gelen kollektif özelliklerinin gerçekleştirilmesine izin verirler. Bu çalışmada sistein molekülü bir bağlayıcı molekül olarak kullanılmıştır. Altın nanoçubuk çözeltisine sistein'in kontrollü eklenmesi altın nanoçubukların iki ucuna tercihli bağlanımına ve altın nanozincir oluşumuna sebep olmuştur. Diğer taraftan altın nanokürelerin kullanımı, sistein moleküllerinin yardımcı hidrojen bağları ile altın nanokümelerin oluşmasına sebep olmuştur. Dizilim oluşumu, UV-vis spektrometrisi ve Alan Emisyonlu- Taramalı Elektron Mikroskopisi ile takip edilmiştir.

Sistein, tiol grubu içeren bir amino asittir ve sistein eksikliği ciddi sağlık problemlerine sebep olmaktadır. Bu yüzden, sistein tayini önemli bir konudur. Burada biz altın nanoparçacıklarının plazmonlarının örtüşmesinden yararlanarak mikromolar konsantrasyondaki sistein'in nicel tayini için iki farklı strateji sunuyoruz. Bunlardan biri yeni yayınlanmış kolorimetrik yöntem ve diğeri ise YGRS metodudur.

Anahtar Kelimeler: Sistein, Altın, Gümüş, Nanoparçacık, Nanoçubuk, YGRS.

To My Future Wife and My Parents

ACKNOWLEDGEMENTS

I would like to express my sincere thanks to my supervisor Prof. Dr. Mürvet Volkan for her guidance, supports and encouragement.

I am deeply grateful to Seher Karabıçak for her endless help, support and frienship. Whenever I need she is always there. I have learned lots of things from her.

I would like to thank Özge Kurtuluş for her endless help, friendship, patience and trust.

I would like to thank all C-50 members; Üzeyir Doğan, Gülfem Aygar, Dilek Ünal, Tuğbanur Alp, Zeynep Ergül, Yeliz Akpınar, and Ceren Uzun. for their help, support and friendship.

I would like to thank all Ataman's research group for their friendship, support and help.

I would like to thank my home-mate Muhammet Tanç for his help, friendship, patience and trust.

I would like to thank my colleagues Semra Saçıcı and Eray Şentürk for their help, support, patience and friendship.

I would like to thank my examination committee members for their time and interest in my MS thesis.

I would like to thank my family for their trust, patience, support and love.

Finally, my special and emotional thanks go to my dear Sema Topal. She gave me incredible support during my thesis period. I felt great emotions thanks to her.

TABLE OF CONTENTS

LIST OF TABLES

LIST OF FIGURES

CHAPTERS

CHAPTER 1

1. INTRODUCTION

1.1 Nano-science

Nano-science is an art of “making, manipulating, and imaging” having very tiny dimensions between 1 to 100 nm (Ozin & Arsenault, 2009; Nagarajan, 2008). Unique optical, physical, chemical, mechanical and electrical properties of materials make nanoscience is an active research area (Nanoparticles and their Applications, 2007).

The nanotechnology is a branch of science which deals with the materials that are ultrasmall particles in the size of nanometer order seen in Figure 1. Nanometer (nm) is used for the length and one nm is extremely small length corresponding to one billionth of one meter. The minus ninth power of ten has a prefix called as “Nano”. The particles with size between 1-100 nm can be called as nanoparticles and a bit bigger particles are accepted as submicron particles, moreover, the lower limit of the wavelength of the visible light could be taken as a measure of nanoparticles (400 nm) (Eustis & El Sayed, 2006).

Nanomaterials with different origins are separated from bulk materials with their many novel properties (Wu, He, & Jiang, 2008). Nanomaterials are also found in various compositions such as metals (Chen, Sorensen, Klabunde, & Hadjipanayis, 1995), metal oxides (Sue, et al., 2006), semiconductors, polymers (Bisht, et al.,

2007), carbon materials (Harris, 1999), organics (Fu & Yao, 2001), or biological materials (Rozhkova, Ulasov, Lai, Dimitrijevic, Lesniak, & Rajh, 2009).

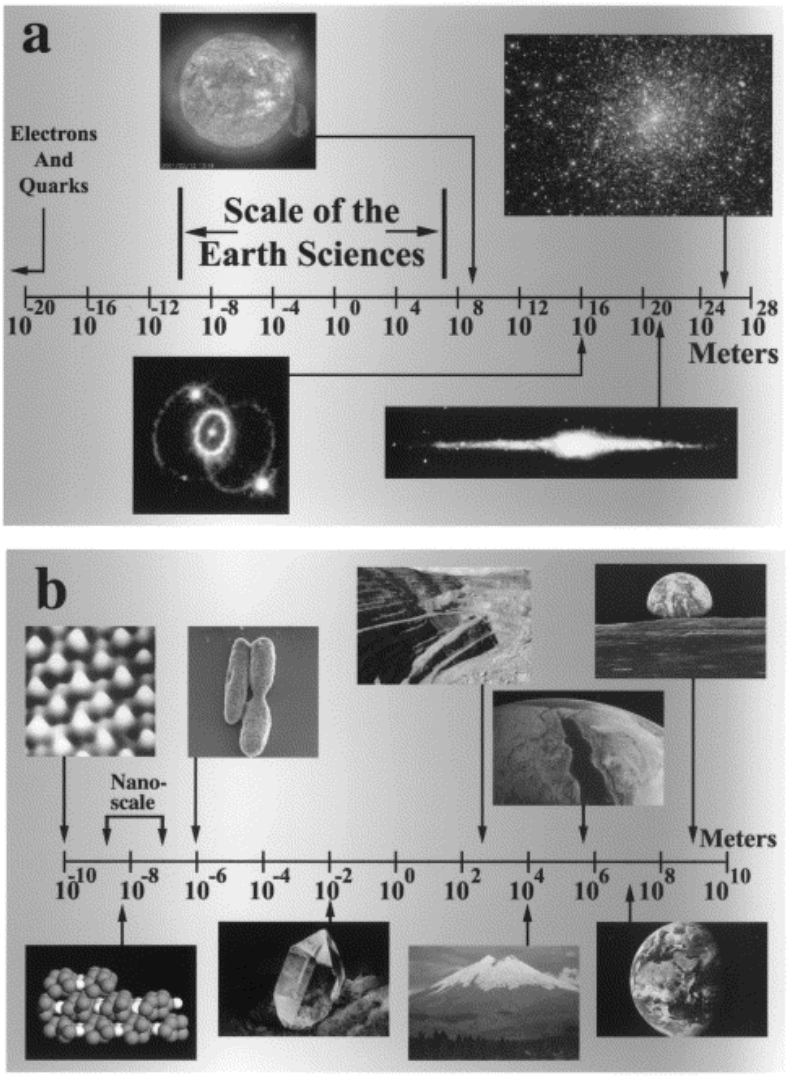

Figure 1 Nano-science is the study of matter at the dimension of 1-100 nm.

Eustis & El Sayed (2006) state that the size of the atom determines the number of atoms in a particle and it results in the specific surface area. On the other hand, the specific surface area of particle drastically increases as the size of the particle lessened. As in the case, if the particle size is lessened from 1 mm to 10 nm, the specific surface area gets larger than $1x10^{10}$ times. As a result of the change in

specific surface area, such properties like the homogeneity and reaction rates are affected. It is one of the main reasons for the difference between bulk and nanomaterials.

In the literature, the main issue in nanotechnology is the difficulty of nanomaterial synthesis and the production of appropriate shape; size and monodispersity of nanoparticles draw attention to develop new techniques. Production of nanomaterials with desired physical and chemical properties needs specific production techniques. As shown in Figure 2, synthesised nanomaterials had different shapes depending upon production techniques (Xia & Halas, 2005).

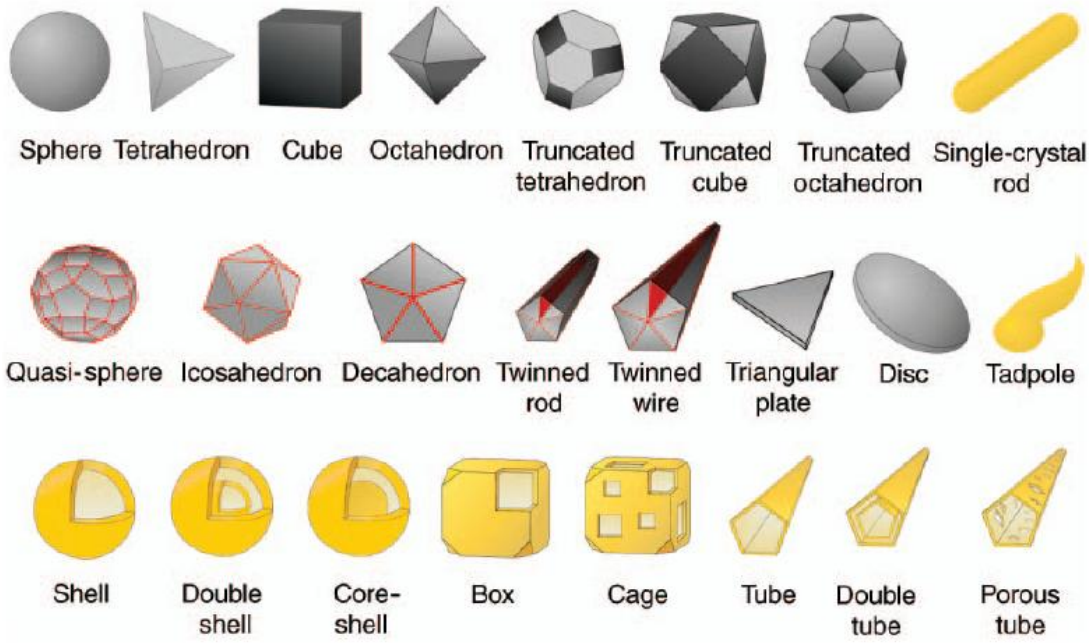

Figure 2 Schematix representations of some gold and silver nanostructures. Yellow shapes represent gold partices, and gray shapes shapes represent silver particles, and also spheres, twinned rods, icosahedrons, and cubes can also be made from gold.

1.2 Nanoparticles

Nanoparticles with different morphologies have drastic changes from their bulk properties (Nikoobakht & El-Sayed, 2003; Alivisatos, 1996; Nie & Emory, 1997; Schmid, 1992). Noble metal nanostructures draw a huge attention with their physical and chemical properties with respect to other nanomaterials. Nobel metal nanoparticles with tunable optical properties are used in catalysis (Nikoobakht & El Sayed, 2001), biosensing (Cullum & Vo-Dinh, 2001), bioimaging (Schultz, 2003), optics (Eychmüller, 2000), optical data storage (Chon, Bullen, Zijlstra, & Gu, 2007) and controlled gene delivery (Salem, Searson, & Leong, 2003). The noble metal nanoparticles such as gold, silver illustrate clear colors because of their surface plasmon resonances (SPR) (Abid, Abid, Bauer, Girault, & Brevet, 2007).

Preparations of one dimensional nanostructures have gained huge attention because of their shape-dependent optical properties. Gold nanoparticles with different shapes have been synthesized and investigated such as spheres (Sokolov, Follen, Aaron, Pavlova, & Malpica, 2003), shells (Loo, Lowery, Halas, West, & Drezek, 2005), rods (Javier, Nitin, Roblyer, & Richards, 2008; Yu, Nakshatri, & Irudayaraj, 2007; Eghtedari, Oraevsky, Copland, Kotov, Conjusteau, & Motamedi, 2007; Huff, Hansen, Zhao, Cheng, & Wei, 2007; Chen, et al., 2006; Liao & Hafner, 2005; Wang, et al., 2005), cages (Cang, et al., 2005; Skrabalak, Chen, Au, Lu, Li, & Xia, 2007) and stars (Nehl, Liao, & Hafner, 2006).

The studies on the SPR absorption of nanomaterials create a big research area to examine properties in nanometer sizes (Noguez, 2007) and the color of metal nanoparticles is found to depend on the shape and size of the nanoparticle and dielectric constant of the surrounding medium, leading to many studies on their synthesis and applications. Studies seek to identify the characteristics of nanoparticles, contributing to the basic science in a manner that creates the ability to use nanoparticles for many applications (Eustis & El Sayed, 2006).

As the morphology of the nanoparticle changes, the color of solution also changes. Gold nanospheres solution has a red color and silver nanospheres solution is yellow.

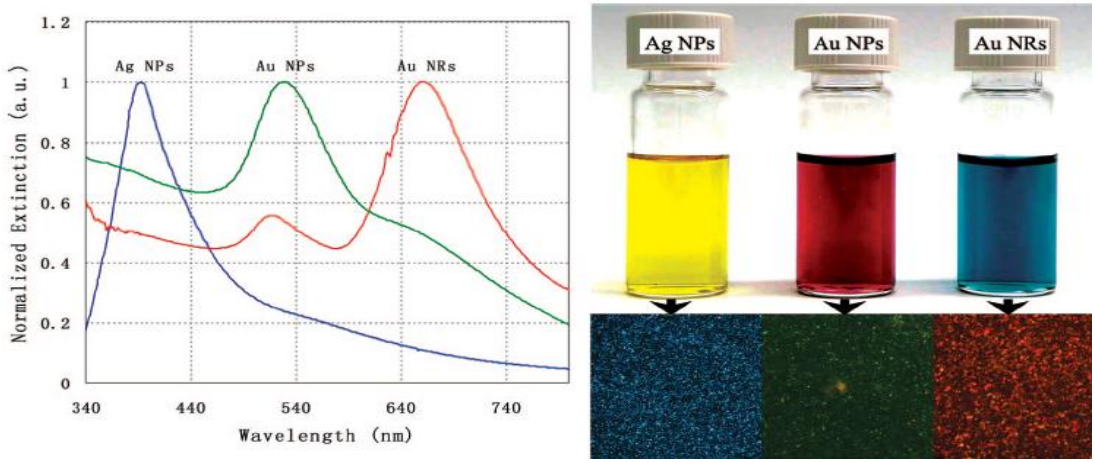

Figure 3 Absorption spectra of gold nanorods (Au NRs), gold nanoparticles (Au NPs), and silver nanoparticles (Ag NPs) and their light scattering images (Eustis & El Sayed, 2006).

The color is due to the collective oscillation of the electrons in the conduction band, known as the surface plasmon oscillation shown in Figure 4. The oscillation frequency is usually in the visible region for gold and silver giving rise to the strong surface plasmon resonance absorption (Eustis & El Sayed, 2006).

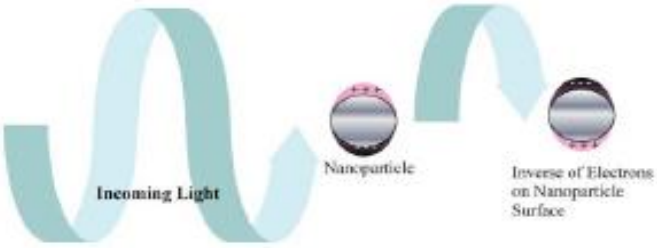

Figure 4 Interaction of the electrons in the conduction band of noble metals with light.

1.2.1 Gold and Silver Nanoparticles

One of the most fascinating aspects of nanosized metal structures is their optical property that finds various technological applications such as SPR detection and imaging, SERS, and biomedical imaging and therapy. Control of the structure and thereby optical properties of gold and silver nanomaterials is especially important for SERS applications because the SERS enhancement factor depends on the optical absorption of the substrate.

Gold and silver exhibits strong absorption in the visible region of the spectrum and is mainly determined by their surface plasmon resonances which shown in Figure 3. After absorption of the incident light, the localized surface plasmon decays radiatively resulting in scattering. So, a strong absorption maximum around 520 nm is observed for aqueous solution of gold nanospheres with particle size around 10 nm in diameter due to their LSPR (Olson Y. , Schwartzberg, Orme, Talley, O'Connell, & Zhang, 2008).Whereas Silver nanoparticles show a surface plasmon absorption peak at 400 nm. When spherical silver nanoparticles exhibit yellow color, colloidal silver nanoparticals which contain spheres, rods and other shapes exhibit a yellowish gray color.

1.2.2 Gold Nanorods

As we know that gold and silver nanoparticles with different morphology have been prepared and among them, nanorods have collected the most attention, because of their controllable preparation (Yang & Cui, 2008), a large number of different production methods (Perez-Juste, Pastoriza-Santos, Liz-Marzan, & Mulvaney, 2005), high yields with nearly same aspect ratio (Busbee, Obare, & Murphy, 2003; Wu, Huang, & Huang, 2007), mild reaction medium (Jana, 2005) and the controllable shape and size result in the change their optical properties (Huang, Neretina, & El

Sayed, 2009; Jana, Gearheart, & Murphy, 2001; Yang & Cui, 2008). Gold nanorods exhibit rich surface plasmon resonance derived properties, which have made discrete nanorods useful for many applications.

Gold nanorods with their anisotropy in dimensions, Figure 5, give rise to a transverse and a longitudinal surface plasmon resonance in the visible-near-infrared region shown in (Placido, et al., 2009; Rostro-Kohanloo, et al., 2009). Owing to surface plasmon resonance, gold nanorods show greatly enhanced absorption and Rayleigh scattering of light (Bouhelier, Beversluis, & Novotny, 2003; Bouhelier, Beversluis, & Novotny, 2003).

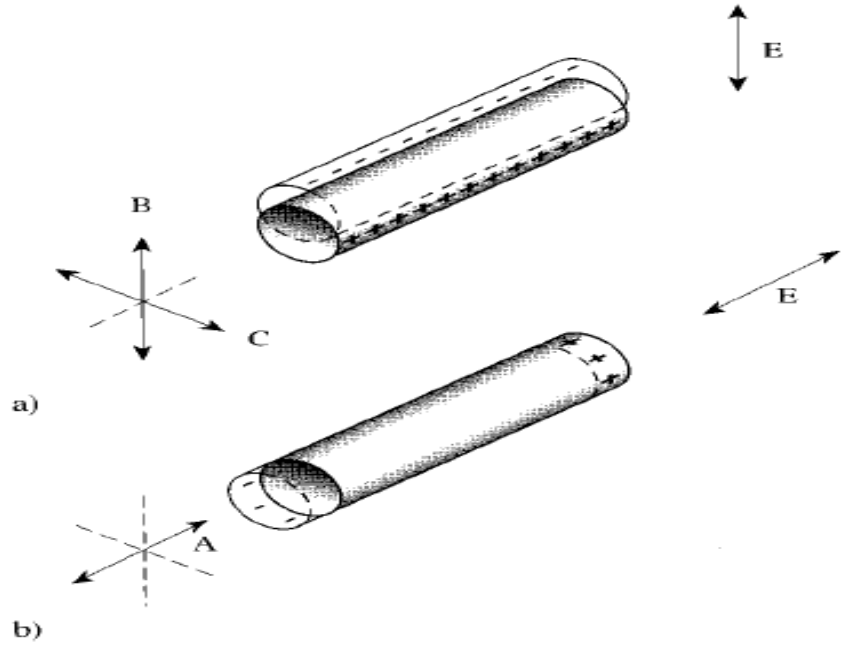

Figure 5 Schematic representation of the surface plasmon resonance in anisotropic particles. E is the oscillating electric field of the incident light. For a rodlike particle, two oscillation modes are possible: (a) the transverse oscillation (along the B or C axis) and (b) the longitudinal oscillation (along the A axis). The plasmon oscillation induces a dipole by local, temporary charge separation (van der Zande, Bohmer, Fokkink, & Schonenberger, 2000).

There are two surface plasmon peaks of gold nanorods unlike from spherical gold nanoparticles. Transverse surface plasmon resonance (TSPR) of gold nanorods located at 520 nm due to end points of rods and it does not depend on the aspect ratio. Spherical gold nanoparticles have same SPR wavelength (520 nm) with TSPR of gold nanorods (Murphy & Jana, 2002). Longitudional surface plasmon resonance (LSPR) of gold nanorods located at near infrared region due to longitudional plasmon oscillations. As the aspect ratio of gold nanorod increases, the longitudional surface plasmon bands shifts to lower energy bands shown in Figure 3 (Miranda, Dollahon, & Ahmadi, 2006).

The aspect ratio is defined as the length of the major axis divided by the width of the minor axis. Thus, "nanospheres" have an aspect ratio of 1 and Murphy (2002) stated that "nanorods" as materials that have a width of ~ 1-100 nm and aspect ratios greater than 1 but less than 20; and "nanowires" analogous materials that have aspect ratios greater than 20.

Application of surface plasmon resonance has occured in sensor technology, in the characterization of molecules at a dielectric-metal interface (van der Zande, Böhmer, Fokkink, & Schönenberger, 1997), in extremely sensitive surface enhanced Raman scattering (Haes, Zou, Schatz, & Van Duyne, 2004) and in plasmonic devices (Nie & Emory, 1997)

1.2.2.1 Synthesis Techniques of Gold Nanorods

In the synthesis of gold nanorods, controlling the shape and size is very important and it is a challenging task. There are several synthetic methods exist for preparing metallic nanorods, such as electrochemical deposition in hard templates such as porous alumina templates (Yu, Chang, Lee, & Wang, 1997; Esumi, Matsuhisa, & Torigoe, 1995), polycarbonate membrane templates (Martin, et al., 1999), and carbon nanotube templates (van der Zande, Bohmer, Fokkink, & Schonenberger, 2000),

electrochemical synthesis in solution (Ying, Chang, Lee, & Wang, 1997), photochemical synthesis (Kim, Song, & Yang, 2002), microwave heating (Liu, Chang, Ko, & Chu, 2004), and seed-mediated growth approach to make varied aspect ratio gold nanorods (Jana, Gearheart, & Murphy, 2001; Gole & Murphy, 2004; Nikoobakht & El-Sayed, 2003). Among these preparation techniques, seed mediated technique is more dominant.

Seed-mediated growth approach was developed by Murphy and co-workers (2005) for producing metallic nanorods in aqueous solution at or near room temperature. Synthesis of gold nanorods takes place in two steps (Murphy & Jana, 2002). The first step is preparation of gold seed nanoparticles. There are many different methods to produce seeds and mostly citrate reduced gold seed and borohydride reduced gold seeds are used in literature (Jana, Gearheart, & Murphy, 2001; Nikoobakht & El-Sayed, 2003).

In the second step of gold nanorods synthesis is the preparation of growth solution which is composed of a rodlike micellar template, CTAB, solution having gold salt, silver salt and a mild reducing agent, ascorbic acid (AA). Synthesized gold seed solution is added to growth solution. Without gold seed addition, no gold nanoparticle formation present in the growth solution.

It has been stated that, silver (I) assisted seed mediated growth technique is more favorable upon synthesis of homogeneous gold nanorods. The equilibrium molar concentration of silver nitrate has an unresolved relationship with the growth of gold nanorods. However, without using silver nitrate, gold nanorods were formed in a wide size range and in low yield Jana et al. (2001) (Nikoobakht & El-Sayed, 2003).

The general formula of the surfactant is given as C_nTAB where n changes as 10 (decyl), 12 (dodecyl), 14 (myristyl), and 16 (cetyl). The critical micelle concentration of C_nTAB in aqueous solution decreases logarithmically with the carbon number in

the tail (from mM for *n*= 10 to 10 μM for *n*= 16). Polar headgroups of CTAB molecule are shown in Figure 6.

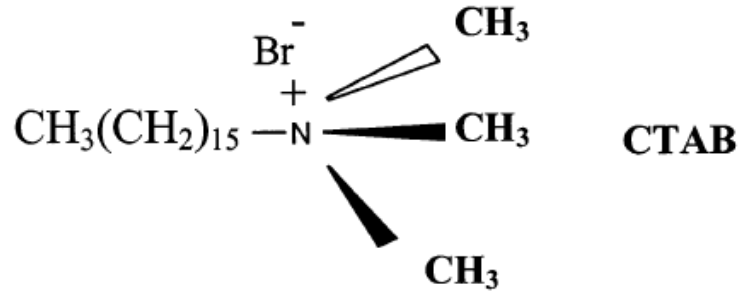

Figure 6 Hexadecyltrimethylammonium bromide (CTAB) (Nikoobakht & El-Sayed, 2003)

CTAB is known as a rod directing surfactant. This fact was explained through its adsorption behavior. El-Sayed and co-workers (2001) have suggested that the CTAB binding takes place via the metal- Br-surfactant complex formation. They have stated that the bromide ion is the bridge between the metal surface having high electron density and the electron deficient quaternary nitrogen of the head groups (Nikoobakht & El Sayed, 2001). C_{16}TAB forms bilayers on gold nanorods, with the positively charged trimethylammonium bromide head group of one monolayer facing the silver surface and the other facing the solvent to maintain water solubility (Gao, Bender, & Murphy, 2003) as shown in Figure 7.

Once the seed grows to a critical size, the facets become large enough for significant surfactant binding. The growth rate of different facets in the presence of the surfactant determines the final shape of the nanoparticle. The slower growth in the NR width is an example of better protection of side {110} facets by CTAB. However, the exact mechanisms by which the growth proceeds are stil not rigorously worked out (Jana, Gearheart, & Murphy, 2001).

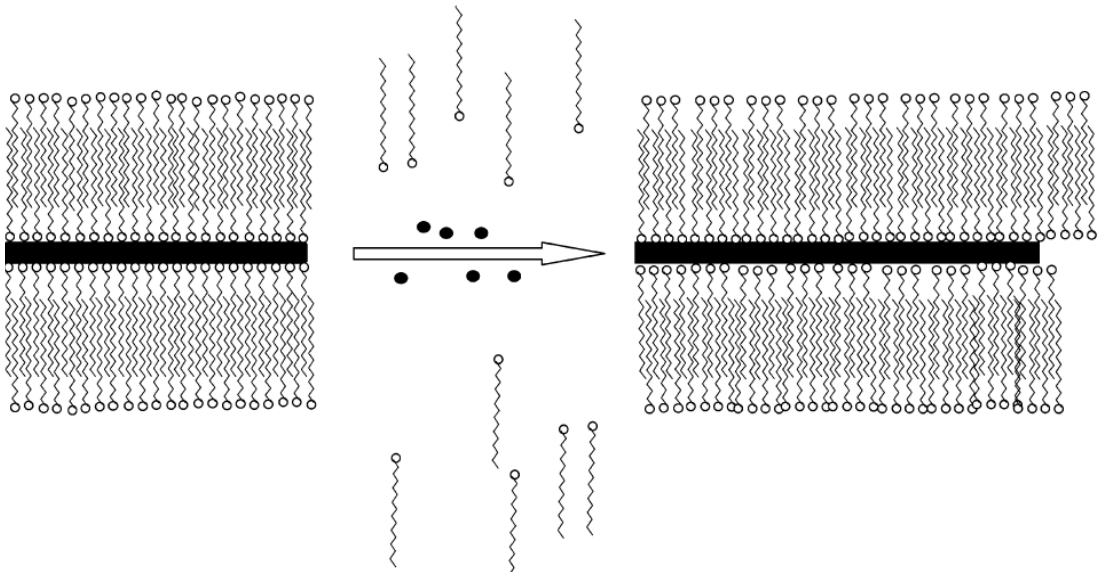

Figure 7 Gold nanorod formation is done in surfactant CTAB. CTAB molecules form double layer on the nanorod surface and assist nanorod formation (Gao, Bender, & Murphy, 2003).

1.2.3 Gold – Silver Core-Shell Nanorods

There are large number of publication regarding the successful and reproducible preparation of silver nanostructures such as spheres, cubes, and stars (Wiley, et al., 2007) (Yang, Matsubara, Xiong, Hayakawa, & Nogami, 2007) (Tan, Li, & Zhu, 2003) (Pyatenko, Yamaguchi, & Suzuki, 2007). However, a reproducible synthesis method for producing high yield of uniform silver nanorods has not been discovered yet. Usually some separation techniques are used to isolate silver nanorods from the silver colloid solution (Lee, Shin, Kim, & Oh, 2004) (Jana, Gearheart, & Murphy, 2001). Everything mentioned above encourages the idea of using gold nanorods as an intermediate template for the following deposition of silver monolayer.

During gold nanorod production, large amount of silver salt was used and there is no silver nanoparticle deposition was observed (Jiang & Pileni, 2007). After 3 years later gold nanorod papers, under alkalic conditions reduction of silver nitrate by ascorbic acid on gold nanorods was observed. Fast depotion of silver atoms on the

gold nanorods result in the dumbbell shaped gold silver nanorods (Liu & Guyot Sionnest, 2004). Under basic conditions, PVP or glycine was used to produce gold silver core shell nanorod production. On the other hand, homogeneous gold silver core shell nanorod production is still a challenging task and if parameters did not controlled carefully many different structures formed unlike nanorods.

1.3 End to End Assembly Self Assembly of Nanoparticles

Application of metal nanoparticles to next generation scientific studies require new designs and improvements in their assembly to more complicated structures (Sun, Ni, Yang, Kou, Li, & Wang, 2008). Therefore nanoparticles should be studied in more than one dimension. Optical and electronic properties of noble metal nanoparticles allow enhancing their collective properties among neighboring monodisperse particles in the assembly of them.

Gold nanoparticles and silver nanoparticles form aggeragetes with linker molecules or high concentration anions. Recent studies showed that assembly of gold nanorods with different linker molecules either end-to-end or side-by-side arrays. These clusters create an electromagnetic enhancement and this enhancement increases as the gap between the nanoparticles decrease. The origin of this effect has been the subject of intense debate. Prevailing theories attribute the origin of the SERS signal as a “hot spot” at the junction of two or more particles.

Well ordered assembly of gold nanorods was done through electrostatic interactions, covalent bonding, or hydrogen bonding (Thomas, Barazzouk, Ipe, Joseph, & Kamat, 2004; Zhang, et al., 2007), antigen/antibody and biotin/streptavidin biorecognition (Caswell, Wilson, Bunz, & Murphy, 2003; Chang, Wu, Chen, Ling, & Tan, 2005), surface modification with polymers in solvents (Park, Lim, Chung, & Mirkin, 2004; Nie, Fava, Kumacheva, Zou, Walker, & Rubinstein, 2007) and using carbon or silica

nanostructures as template (Hazarika, Ceyhan, & Niemeyer, 2004; Sharma, Chhabra, Liu, Ke, & Yan, 2006).

Surface coverage of CTAB is not regular at the end points of the gold nanorods and the nanorods are binded to each other from these end points with linker molecules. Sulfur containing molecules are preferentially binded to gold atoms via S-Au bond (Aryal, Remant, Dharmaraj, Bhattarai, Kim, & Kim, 2006) .

The longitudional surface plasmon resonance absorption bonds of gold nanorods coupled with each other when gold nanorods are assembled, and longitudional surface plasmon peak is red shifted.

1.4 Detection of Cysteine

The lack of cysteine can result in slow growth, hair depigmentation, edema, weakness, lethargy, liver damage, skin lesions, and muscle and fat lost (Li, Wu, Zheng, Lai, Zhang, & and Zhao, 2010; Rusin O. , et al., 2004). The detection of cysteine has been studied by many research groups and most of them used redox chemistry or derivarization with fluorophores or chromophores (Rusin O. , et al., 2004). Thiol groups of amino acids are also examined with high pressure liquid chromatography (HPLC) or capillary electrophoresis separations or via immunoassays. Therefore, cysteine detection needs more easier and high sensitive techniques (Li, Duan, Liu, & Du, 2006). Thiol functional group of cysteine results in color change with nanoparticles (Zhang, et al., 2002). Therefore colorimetric detection of cysteine by using gold and silver nanoparticles is applicable in their physicological levels qualitatively (Rusin, Luce, & Agbaria, 2004).

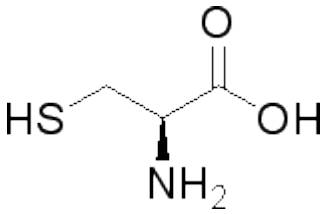

Figure 8 Molecular structure of L-Cysteine (Sigma Aldrich Co., 2011)

Surface enhanced Raman spectroscopy (SERS) is a good analytical tool to detect trace amount of molecules in the medium by using substrates. End to end assembled gold nanorods with linker molecule cysteine is a natural substrate to detect cysteine molecule. Au-S bond formation between gold nanorod and cysteine thiol group occurs only at the tip points of gold nanorods and the cysteine molecules two neighboring gold nanorods enhanced electromagnetically.

1.6 Raman Spectrometry

Raman spectroscopy is a light scattering technique in which a photon of light interacts with a molecule to create scattered radiation (Raman Spectroscopy, no date). In 1928, the phenomenon of inelastic light scattering was noticed and documented by Sir Chandrasekhara Venkata Raman. He won the Nobel Prize in Physics 1930 for his work on the inelastic scattering of light and for the discovery of the effect named after him. Raman spectroscopy has many application areas such as pharmaceuticals, semiconductors, and carbon nanomaterials. It gives rich information about structure of molecule and effects of bonding.

Raman spectroscopy is an analytical method that offers several important advantages. It provides a rapid and non-destructive analytical tool, it yields highly compound-specific information for chemical analysis and it has great potential for multi-component analysis. Aqueous systems can be studied by using Raman spectroscopy. Usually little or no sample preparation is needed. We can obtain a

Raman spectrum in a few seconds and since fundamental modes are measured, Raman bands can be easily related to chemical structure.

One limitation of Raman spectroscopy is its low sensitivity. Inherently not sensitive and it needs ~ one million incident photons to generate one Raman scattered photon. Fluorescence is a common background issue and typical detection limits in the parts per thousand range.

1.6.1 Surface Enhanced Raman Spectroscopy (SERS)

An effect was observed in the early 70's when molecules deposited on rough noble metal surfaces showed greatly enhanced Raman scattering. Rough surfaces are decorated with nanoparticle shapes with surface plasmon oscillations. This effect has come to be known as surface enhanced Raman scattering (SERS). Enhancement in SERS occurs with two mechanisms. These are electromagnetic enhancement and chemical enhancement. Electromagnetic enhancement that is the metal particles become polarized at plasmon frequency, resulting in large field induced polarization, large local field on the surface. Surface plasmons are electromagnetic waves that propagate along the surface parallel to the metal/dielectric interface. Both the incident laser field and scattered Raman field were enhanced due to surface plasmons. The largest enhancements occur for surfaces which have nanostructures which have a size 10‑100 nm.

The Electromagnetic field can be greatly enhanced at the gaps or the junctions between nanostructures, which are often called "hot spots". As the interparticle distance between two nanoparticles decreases, the degree of their surface plasmon coupling increases, and the enhanced fields of each particle begin to interfere coherently at the junctions. Therefore, it is generally understood that in a number of systems, aggregates of nanoparticles are better substrates for SERS applications than individual nanoparticles due to the presence of junctions.

1.7 Aim of This Study

In this study, gold nanorods will be prepared by silver assisted seed mediated surfactant directed growth method and core shell gold silver nanorods will be produced by reduction of silver on the surface of gold nanorods. Synthesized nanostructures will be characterized by UV-vis Spectroscopy, Field Emission-Scanning Electron Microscopy, Energy Dispersive X-ray analysis and High Resolution-Transition Electron Microscopy. Gold nanorod chains and gold nanoparticle clusters will be prepared using cysteine as a linker molecule. Optical and electronic properties of agglomerated gold nanostructures will be examined.
Thus prepared nanostructures will be for the quantitative determination of cysteine.

CHAPTER 2

2. EXPERIMENTAL

2.1 Chemical and Reagents

i) Aurochloric Acid ($HAuCl_4$, 99%), has been purchased from Sigma Aldrich, Germany.

ii) Sodium Borohydride ($NaBH_4$, 96%), has been used as a strong reducing agent in seed solution and purchased from Merck KGaA Darmstadt, Germany.

iii) Hexadecyltrimethylammonium Bromide ($CH_3(CH_2)_{15}N(Br)(CH_3)_3$),(CTAB, 97 %), has been used as a soft template of the growth solution and purchased from Sigma Aldrich, Germany.

iv) Silver Nitrate ($AgNO_3$, 97%), has been purchased from Sigma Aldrich, Germany.

v) Ascorbic Acid ($C_6H_8O_6$, 97%), has been used as reducing agent in growth solution and purchased from Sigma Aldrich, Germany.

vi) Concentrated Hydrochloric Acid, (37%,(w/w)), has been purchased from J. T. Baker.

vii) Sodium Hydroxide (NaOH) has been purchased from Sigma Aldrich, Germany.

viii) L-Cysteine (97%), has been purchased from Sigma Aldrich, Germany.

ix) Polyvinylpyrrolidone (PVP), has been purchased from Sigma Aldrich, Germany.

x) Trisodium Citrate ($Na_3(C_6H_5O_7)$, 99%), been purchased from Sigma Aldrich, Germany.

All reagents used in this study were in analytical grade and used without further purification. Dilutions were made using 18 MΩ.cm deionized water obtained from a Millipore (Molsheim, France) Milli-Q water purification system. All the glassware and plastic ware were cleaned by soaking them in 10% HNO_3 for at least 24 hours and then rinsing three times with distilled water and with deionized water.

2.2 Instrumentation

2.2.1 Centrifuge

Sigma 2-16 model centrifuge was used to remove excess reagents from solutions and to separate nanorods from nanospheres.

2.2.2 UV-Visible Spectrophotometer

Varian Cary 100 Bio UV-Visible spectrophotometer was used to follow the optical properties of the nanostructures and plastic cuvettes (10 mm path length) were used in all measurements.

2.2.3 Field Emission Scanning Electron Microscopy (FE-SEM)

For SEM measurements, samples were prepared by dropping 20 μL sample solution on carbon-coated copper grids and drying at room temperature. QUANTA 400F Field Emission scanning electron microscope was operated at 30 kV at high vacuum for SEM measurements at the METU Central Laboratory.

2.2.4 Energy-dispersive X-ray analysis (EDX)

Energy-dispersive X-ray analysis was performed with a scanning electron microscope equipped with energy-dispersive X-ray analyzer (EDAX) at the METU Central Laboratory.

2.2.5 High Resolution Transition Electron Microscopy (HR-TEM)

For TEM measurements, samples were prepared by dropping 2-3 μL sample solution on polycarbon grid with 400 mesh and drying at room temperature.

2.2.6 Surface Enhanced Raman Spectrometer (SERS)

SERS measurements were done with Jobin Yvon LabRam confocal microscopy Raman spectrometer with a charge-coupled device (CCD) detector and a holographic notch filter. It was equipped with an 1800-grooves/mm grating and all measurements were done with a 200 μm entrance slit. SERS excitation was provided by 632.8 nm

radiation from a He-Ne laser with a total power of 20 mW. Acquisition time was 20 second for data collection.

2.3 Synthesis of Nanostructures

2.3.1 Synthesis of Gold Nanoparticles

Gold nanoparticles (gold NPs) were synthesized by a sodium citrate reduction method (Frens, 1973). Fifty milliliters of $2.5x10^{-4}$ M $HAuCl_4$ was brought to a boil. To make 34±3 nm and 22±3 nm gold NPs, 0.5 and 0.74 mL of 1% sodium citrate was added to the boiling gold salt solution, respectively. The solution was boiled until the color was turned to ruby red (Olson R. Y., Schwartzberg, Orme, Talley, O'Connell, & Zhang, 2008).

2.3.2 Synthesis of Silver Nanoparticles

Silver NPs were synthesized with trisodium citrate as the reducing agent as described by Lee and Meisel (Lee & Meisel, 1982). A 225 mg of silver nitrate was dissolved in 250 mL of water and brought to a boil. To the boiling solution, 5 mL of 1% sodium citrate was added and allowed to continue boiling for 1 h. After 1 h, solution was taken from hot plate and continued to mix at room temperature (Olson R. Y., Schwartzberg, Orme, Talley, O'Connell, & Zhang, 2008).

2.3.3 Synthesis of Gold Nanorods

In the synthesis of homogeneous gold nanorods, we preferred to use silver-assisted surfactant-directed seed mediated growth technique shown in figure 9. In this technique, gold nanoseeds were produced by a strong reducing agent and growth of gold nanorods were done by addition of more gold salt, silver salt, a mild reducing agent, and gold seed solution in the presence of directing surfactant.

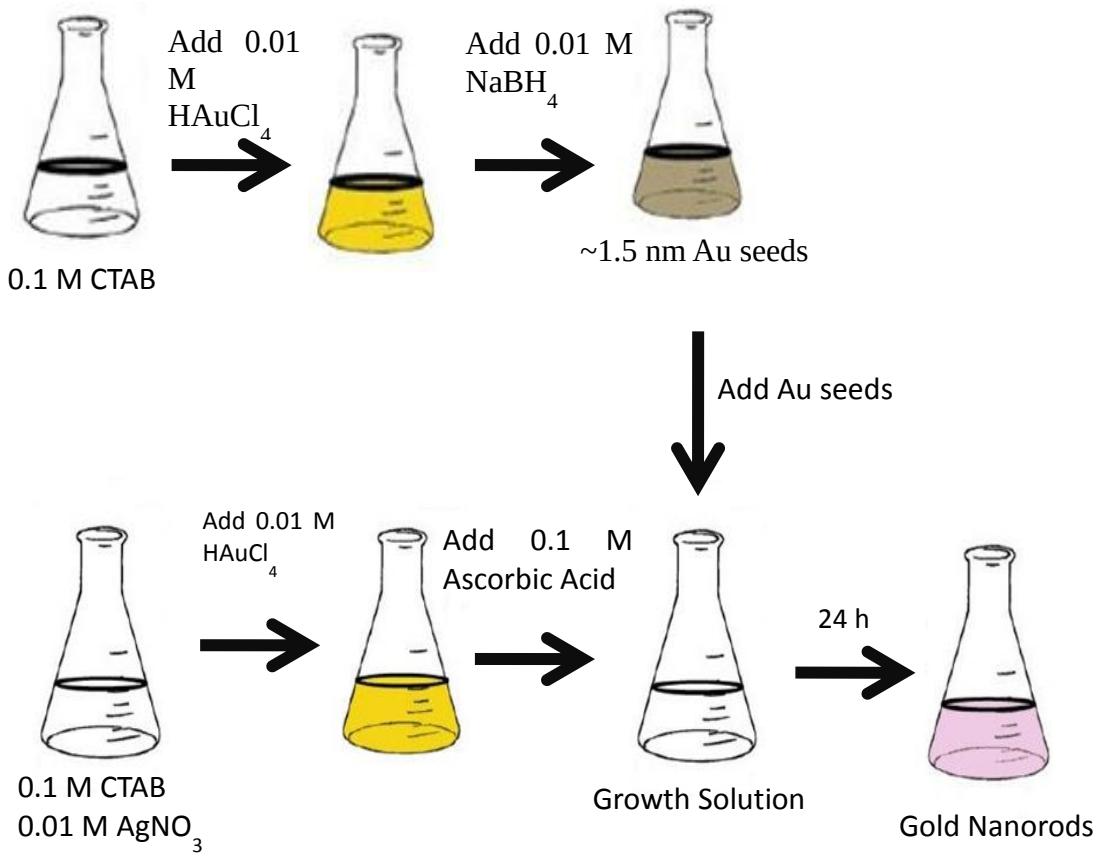

Figure 9 Synthesis of Gold nanorods by using Silver (I) assisted seed mediated growth technique.

2.3.3.1 Preparation of Gold Seed Solution

The nanospheres were synthesized with slightly modifications according to a general procedure which has been reported by Murphy and co-workers (Gou & Murphy, 2005; Jana, Gearheart, & Murphy, 2001; Gole & Murphy, 2004). A seed solution of gold colloid was prepared by mixing 4.875 mL of a 0.1M CTAB solution with 0.125 mL of an aqueous 0.010 M solution of $HAuCl_4$ and stirred gently. The solution appeared dark yellow in color. To the stirred solution, 0.300 mL of an aqueous 0.010 M ice-cold $NaBH_4$ solution was added all at once, followed by sonication mixing for

3 minutes. Care should be taken to allow the escape of the evolved gas during incubation. The color of the solution turned to a pale brown-yellow color. The solution is ready to use after 2 h. This seed was used 2 hour after preparation but could not be used after 5 hours; the seed solution should not be used if the color of solution turned pink.

2.3.3.2 Preparation of Growth Solution

An aqueous growth solution was prepared by combining 4.75 mL of 0.10 M CTAB, 50 μL of 10 mM $AgNO_3$, and 250 μL of 0.010 M $HAuCl_4$. The color of the stock solution was dark yellow and after the addition of a 44 μL of 0.10 M ascorbic acid, the color of stock solution was changed to colorless. The prepared stock solution is waited 10 minutes and then it is ready to use in gold nanorod synthesis.

2.3.3.3 Production of Gold Nanorods in Solution Phase

Prepared growth stock solution was mixed with 6.0 μL of gold seed solution and mixed by capping the reaction vessel and slowly inverting it two times. After seed addition, the growth solution was maintained at 25-30 ^{o}C without stirring overnight.

2.3.4 Synthesis of Gold-Silver Core-Shell Nanorods

Liu and Guyot-Sionnest (2004) reported a fast and short procedure to prepare gold core silver shell nanorods with tunable optical properties. According to this procedure, 0.80 ml of synthesized gold nanorod solution was taken and added to 4.0 ml 1% PVP solution. Silver shell formation on gold nanorods was done by reduction of silver nitrate by using ascorbic acid under alkaline conditions. Optical properties of gold core silver shell nanorods changed with silver shell thickness were controlled by changing reagents' concentrations (Khlebtsov, Khanadeev, Bogatyrev, Dykman, & Khlebtsov, 2009).

2.4 Optimizations of Nanostructures

Parameters which affect the nanostructures' size, shape and morphology were adjusted during the study to have better structures and properties.

2.4.1 Optimization of Gold Colloid Solution

Optimization of gold nanospheres was done by varying the concentration of sodium citrate added to gold salt solution without changing amount of gold salt.

2.4.2 Optimization of Silver Colloid Solution

Optimization of silver nanoparticles was done by varying the concentration of sodium citrate added to silver salt solution without changing amount of silver salt.

2.4.3 Optimization of Gold Nanorod Solution

Gold nanorods were prepared by controlling many parameters. Adjusted parameters are gold seed preparation, CTAB concentration, silver nitrate concentration, ascorbic acid concentration, volume of added gold seed, ageing time of growth solution for the formation of nanorods, and addition sequence of the reagents.

2.4.3.1 Optimization of gold seed solution

In seed mediated growth approach, there are different seed preparation techniques and they have many application fields. In the synthesis of gold nanorods, we have examined two of them which are citrate stabilized gold seeds and CTAB capped gold seeds.

2.4.3.1.1 Preparation of citrate stabilized gold seed solution

Gold seed solution was prepared with respect to Gole's method (2004). In this method, negatively charged gold nanoparticle seeds were prepared within 20.0 ml aqueous solution of 2.50×10^{-4} M $HAuCl_4$ and 2.50×10^{-4} M trisodium citrate by addition of 600 µl ice cold 0.10 M $NaBH_4$. After $NaBH_4$ addition, color of solution turned to reddish-orange, solution mixed for 30 second and then seed solution was

kept at 30 ^{o}C for 2 hour before using in rod synthesis. After 2 hour, H_2 gas exhalation was completed and negatively charged citrate capped gold seeds (~3.5 nm) are ready to further use.

2.4.3.1.2 Preparation of cationic CTAB capped gold seed solution

The procedure was described previously and in this technique, the nanospheres were synthesized with slightly modifications according to a general procedure which has been reported by Murphy and co-workers (Gou & Murphy, 2005; Jana, Gearheart, & Murphy, 2001; Gole & Murphy, 2004). A seed solution of gold colloid was prepared by mixing 4.875 mL of a 0.1 M CTAB solution with 0.125 mL of an aqueous 0.010 M solution of $HAuCl_4$ and stirred gently. The solution appeared dark yellow in color. To the stirred solution, 0.300 mL of an aqueous 0.010 M ice-cold $NaBH_4$ solution was added all at once, followed by sonication for 3 minutes. Care should be taken to allow the escape of the evolved gas during incubation. The color of the solution turned to a pale brown-yellow color. The solution is ready to use after 2 h. This seed was used 2 hour after preparation but could not be used after 5 hours; the seed solution should not be used if the color of solution turned pink.

2.4.3.2 Optimization of the Growth Conditions

2.4.3.2.1 Optimization of CTAB

The concentration of CTAB which works as a soft template is an important parameter to produce homogeneous gold nanorods and three different set (0.05 M, 0.10 M, and 0.15 M) of CTAB examined. The surface plasmon bands were followed by UV-Visible spectrophotometer.

During gold nanorod production experiments, CTAB concentration of growth solution is optimized to 0.10 M.

2.4.3.2.2 The effect of equilibrium molar concentration of silver nitrate

The equilibrium molar concentration of silver nitrate has a close relationship with the aspect ratio of gold nanorods. To optimize the concentration of it, 7 different gold nanorod solutions with varied volumes (0 μL, 13 μL, 25 μL, 50 μL, 100 μL, 150 μL, and 250 μL) of 10 mM $AgNO_3$ is used with the same procedure. The surface plasmon bands were followed by UV-Vis spectrophotometer.
During gold nanorod production experiments, volume of 10 mM $AgNO_3$ in growth solution is optimized to 50 μL.

2.4.3.2.3 The effect of equilibrium molar concentration of Ascorbic acid

The mild reducing agent, ascorbic acid has a crucial role to produce homogeneous and smart gold nanorods. Five different set of 0,10 M ascorbic acid with varied volumes (30 μL, 38 μL, 44 μL, 50 μL and 55 μL) is used to optimize gold nanorods. The surface plasmon bands were followed by UV-Visible spectrophotometer.

During gold nanorod production experiments, volume of 0,10 M ascorbic acid in growth solution is optimized to 44 μL.

2.4.3.2.4 The effect of seed addition to the growth solution

The number of nucleation center has a direct relationship with the number of synthesized gold nanorods and their aspect ratios. Therefore, three different sets of experiment are performed with different volumes (3.0 μL, 6.0 μL, and 12.0 μL) of gold seed solution. The surface plasmon bands were followed by UV-Visible spectrophotometer.

During gold nanorod production experiments, volume of CTAB capped gold nanoseed solution in growth solution is optimized to 6.0 μL.

2.4.4 Optimization of Gold Silver Core Shell Nanorod Solution

Optimization of gold- silver core-shell nanorods was done by controlling the silver shell thickness of the nanorods. To do this, firstly gold nanorods were synthesized by using 4.75 mL 0.10 M CTAB with 50 μL 10 mM $AgNO_3$, 250 μL of 0.010 M $HAuCl_4$, 44 μL of 0.10 M ascorbic acid and 6 μL of CTAB capped seed solution and capping the reaction vessel and slowly inverting it two times. After seed addition, the growth solution was maintained at 25-30 ^oC without stirring overnight.

9 set of solutions which contain 0.80 ml of prepared gold nanorod solution and 4.0 mL of 1 % PVP water solution were prepared and varied volume (0-900 μL) of 1 mM silver nitrate solution was added to each set of solution. In 10 minutes, silver shell formation was observed and the surface plasmon bands were followed by UV-visible spectrophotometer.

During gold silver core shell nanorod production experiments, volume of added 1 mM silver nitrate is optimized to 540 μL.

2.5 End-to-end self-assembly of gold nanorods

2.5.1 End-to-end self-assembly of gold nanorods by using l-cysteine

L-cysteine is a thiol containing amino acid and it was attached the end points of gold nanorods more favorably (Aryal, Remant, Dharmaraj, Bhattarai, Kim, & Kim, 2006). In acidic medium, L-cysteine molecules attached to the gold nanorods by using thiol groups form gold nanorod chains by forming hydrogen bonding between carboxyl and amine groups of two neighboring L-cysteine molecules.

According to Sun et al., end to end self-assembly of gold nanorod chains was done with slightly modification (2008). Prepared gold nanorods were centrifugated at 5000 rpm for 20 min. and washed twice. Centrifugated and washed gold nanorods were redispersed in 5 mL water and pH adjusted with 5.00 M HCl and 0.10 M NaOH. 0.10

M aqueous stock solution of L-Cysteine was prepared and added to pH adjusted gold nanorod solution to make final concentration of cysteine 0,10 mM.

The assembly of gold nanorods was carried out in an isothermal water bath at 45 ^{o}C for 2 h.

2.5.2 Optimization of self-assembled gold nanorods.

End to end assembly of gold nanorods is done by cysteine addition and pH adjustment. Therefore, cysteine concentration and pH value should be determined exactly to find optimum conditions.

2.5.2.1 pH optimization of cysteine containing gold nanorod solution

Cysteine is a zwitterionic molecule and at low pH values end to end assembly of gold nanorods is faster. Therefore, 6 set of gold nanorod solution with same concentration of cysteine was prepared and 5.00 M HCl was added to change pH values within 2.00-6.00. The longitudional surface plasmon band was followed by UV-Visible spectrophotometer.

2.5.2.2 Optimization of time dependent gold nanochain formation

End to end well ordered gold nanorod chains were done by cysteine molecules and appropriate number of collion to form gold nanochains depends on the time. To determine the optimum reaction time to assemble gold nanorod chains, the longitudional surface plasmon band was followed by UV-Visible spectrophotometer.

CHAPTER 3

3. RESULTS AND DISCUSSION

In this study, noble metal nanostructures were synthesized and optimized. Characterizations of the particles were done by using UV-vis Spectrophotometry, Energy-dispersive X-ray analysis (EDX), Field Emission-Scanning Electron Microscopy (FE-SEM) and High Resolution-Transmission Electron Microscopy (HR-TEM).

Gold and silver nanoparticles with different shapes and morphologies were used as SERS substrate and their performance were followed by using linker molecule cysteine as model compound.

Amino acid cysteine as a linker molecule was used to end to end assembly of gold nanorod chains. Besides nanorod chain formation, spherical nanoparticles were conjugated by cysteine molecules. Obtained results directed us to use nanoparticle clusters so as to detect cysteine by using SERS technique.

Cys is not only linker molecules but also a Raman active model molecule in this study. Cysteine molecule has 3 functional groups and thiol group of cysteine was followed by SERS measurements. Experimental results from these SERS substrates were listed below.

3.1 Nanostructures

3.1.1 Gold Nanospheres

Gold nanoparticles were synthesized with citrate reduction method (Frens, 1973). Two different gold colloids were synthesized. 0.50 ml of 1% citrate solution added gold solution result in surface plasmon absorption peak at 525 nm gold nanospheres and 0.74 ml of 1% citrate solution added gold solution result in surface plasmon absorption peak 519 nm gold spheres. Their UV-vis absorption profiles were shown in Figure 10. Concentration of added citrate ion determines the size of the gold nanospheres. As expected, increasing concentration of citrate decreases the size of gold nanospheres. SEM image and EDX analysis of 20-25 nm sized nanospheres are shown in Figure 11 and Figure 12, respectively. Gold nanospheres with 22±3 nm size which have a surface plasmon absorption peak at 519 nm were chosen as SERS substrate.

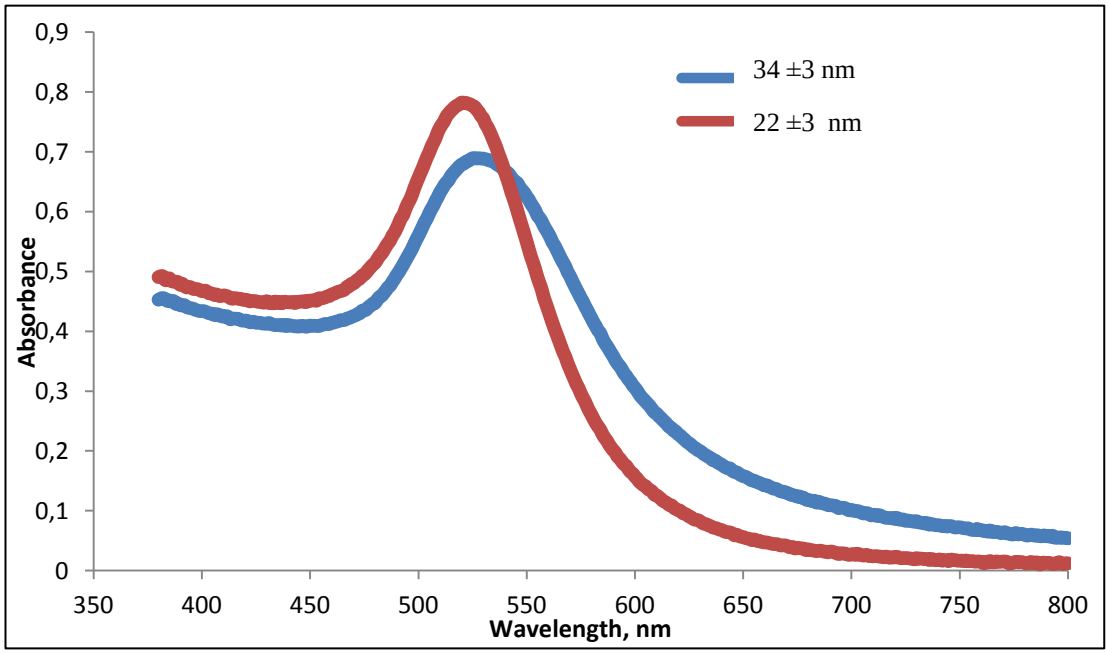

Figure 10 UV-Vis spectra of Au nanospheres. Blue line 34±3 nm sized nanospheres and red line 22±3 nm sized nanospheres.

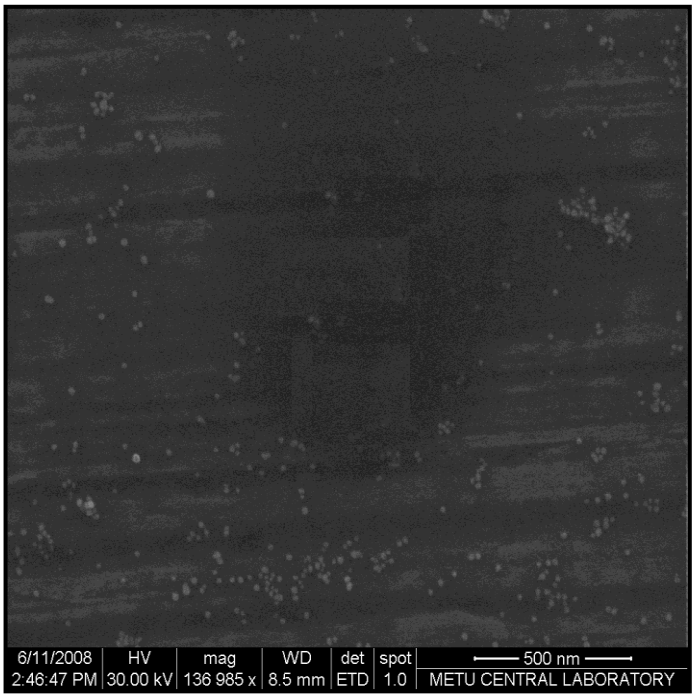

Figure 11 FE-SEM images of gold nanospheres.

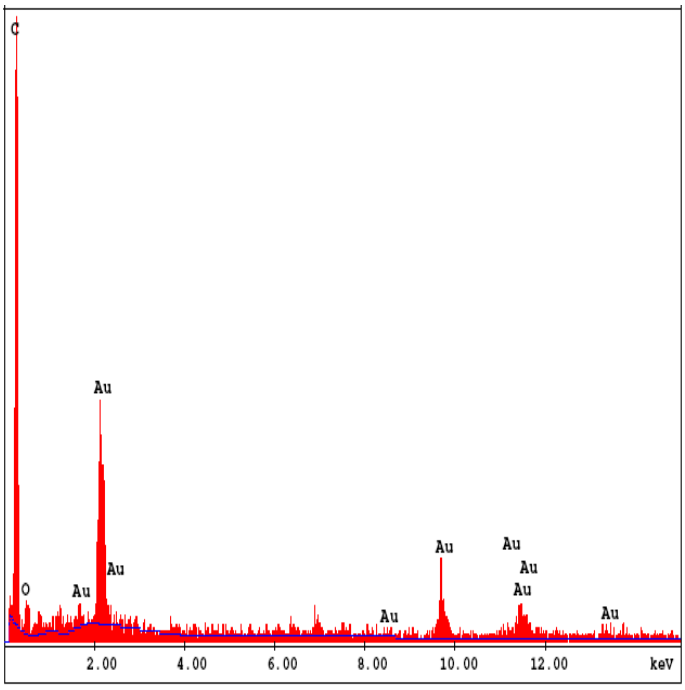

Figure 12 EDX patterns of the gold nanospheres.

3.1.2 Silver Nanoparticles

Silver nanoparticles were synthesized with Lee & Meisel method (Lee & Meisel, 1982). UV-Vis spectrum, SEM image and EDX analysis of silver nanoparticles are given in Figure 13, Figure 14, and Figure 15 respectively. As can be seen from the FE-SEM images, colloid solution contains a mixture of silver spheres, rods and other shapes. As a result of this nanoparticle mixture, a broad surface plasmon peak having a maximum at 435 nm was observed, shown in Figure 13.

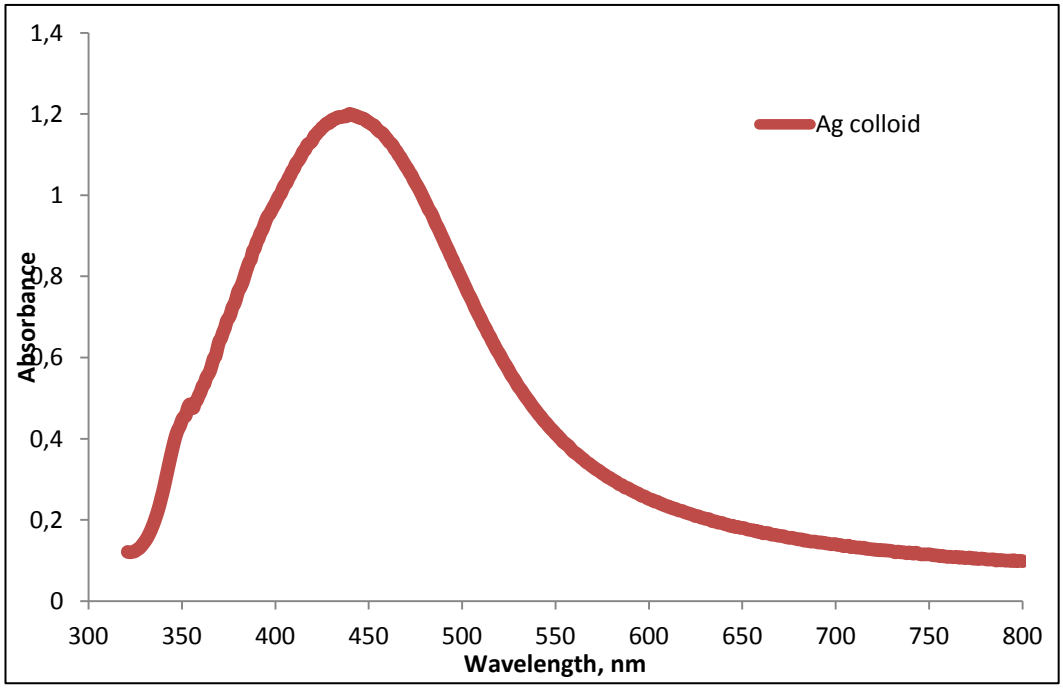

Figure 13 UV-Vis spectra of silver nanoparticles. Surface plasmon absorption peak at 435 nm.

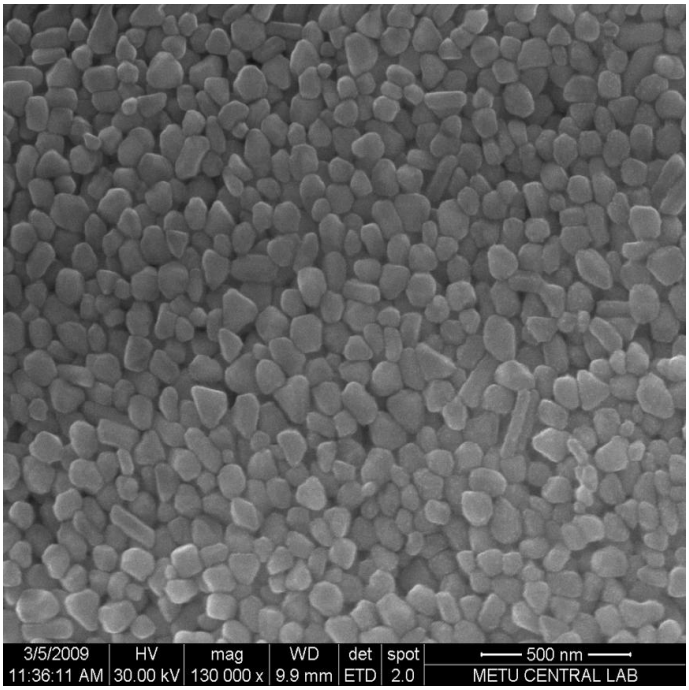

Figure 14 FE-SEM images of silver nanoparticles.

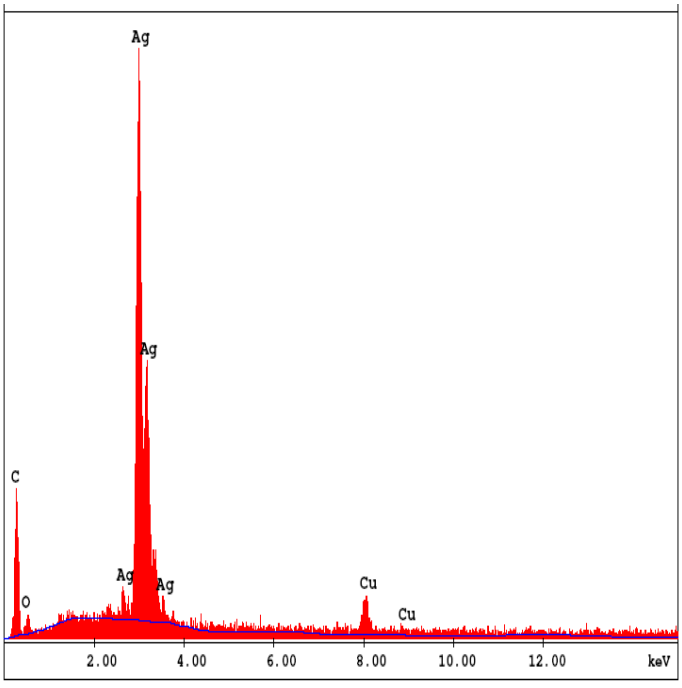

Figure 15 EDX patterns of the silver nanoparticles.

3.1.3 Gold Nanorods

Homogeneous gold nanorods were synthesized in aqueous solution through silver-assisted seed mediated growth technique at room temperature and used as a SERS substrate. In order to obtain gold nanorods with an optimal aspect ratio, parameters such as type of reducing agent used for gold seed preparation, CTAB concentration, silver nitrate concentration, ascorbic acid concentration and volume of added gold seed solution were optimized. The changes in the aspect ratio of the nanoparticles were followed by measuring their surface plasmon absorptions using UV-visible spectrometer. Characterizations of the particles were done using FE-SEM and HR-TEM.

3.1.3.1 Optimization of the seed solution

Synthesis of the gold seeds was done with two different methods (Gole & Murphy, 2004; Jana, Gearheart, & Murphy, 2001). First method is stabilization of gold seeds with negatively charged citrate ions as mentioned in section 3.1.1 Second method is stabilization of gold seeds with positively charged CTAB molecules. Brown color of seed solution with surface plasmon band maximum at 525 nm was obtained. UV-visible absorption profiles of seed solutions stabilized by Citrate and CTAB are shown in Figure 16.

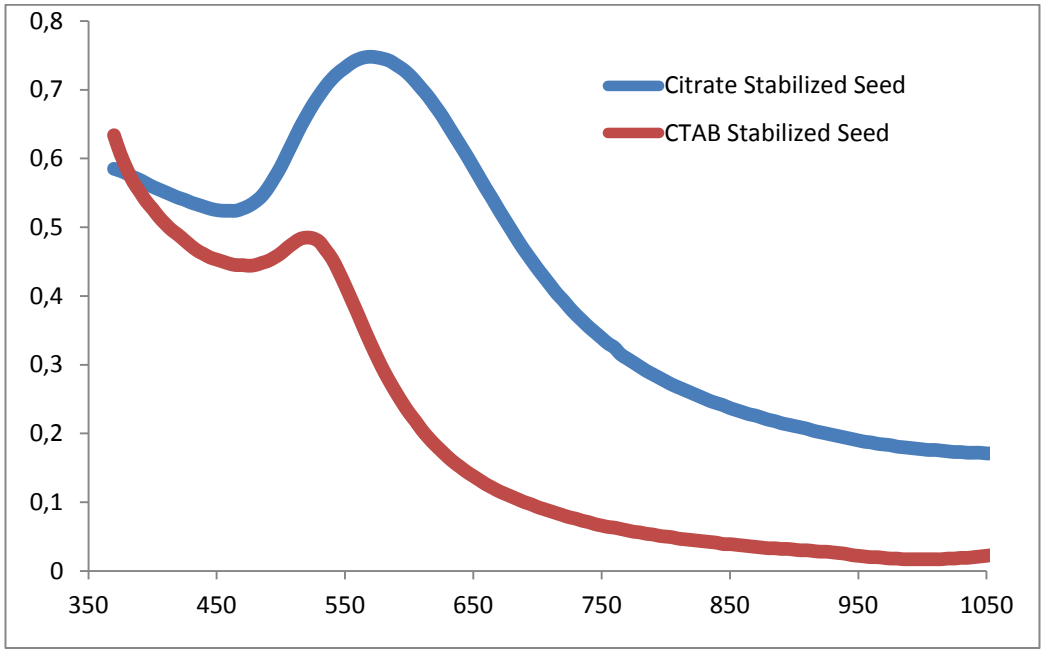

Figure 16 UV-visible absorption profile of seed solutions which stabilized by Citrate and CTAB.

As can be seen from Figure 16, CTAB stabilized gold seeds show a narrow size distribution compared to that of citrate stabilized ones.

These seeds are then added to a growth solution containing additional gold salt, ascorbic acid and CTAB for the nanorod formation. The plasmon bands of gold nanorod solution prepared by citrate stabilized gold seeds and CTAB stabilized gold seeds are shown in Figure 17 and peak positions are stated in Table 1. Appearance of a transverse and a longitudinal surface plasmon resonance in the visible-near-infrared region was expected due to the anisotropy in dimensions of nanorods. Citrate stabilized gold seed solution result in the low yield of gold nanorods and high yields of spherical gold nanoparticles. As a result of this, longitudional surface plasmon bands did not observed in Figure 17. On the other hand, CTAB stabilized gold seed solution produced high yield of gold nanorods.

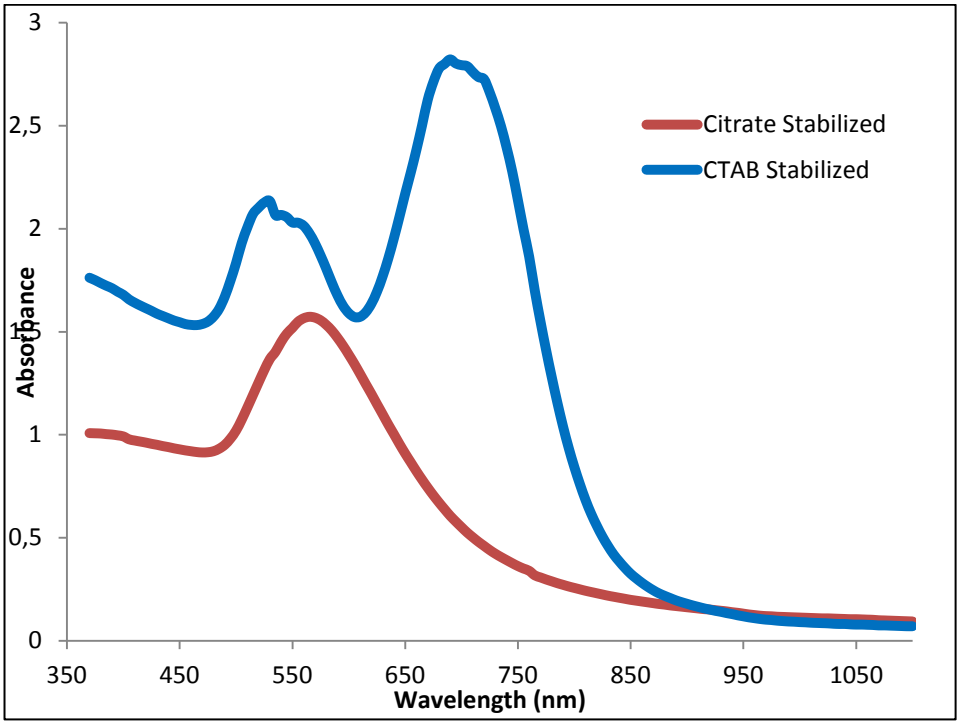

Figure 17 UV-visible absorption profile of gold nanorod solutions which prepared by citrate stabilized seeds and CTAB stabilized seeds.

Table 1 The plasmon bands of gold nanorod solution prepared by citrate stabilized gold seeds and CTAB stabilized gold seeds and with 0.50 mM $HAuCl_4$, 0.1 M CTAB, 0.10 mM $AgNO_3$, 1.0 mM ascorbic acid, and 6 µL seed.

Seed Stabilization	Peak maximum of Transverse Plasmon band, nm	Absorbance value at the peak maximum	Peak maximum of Longitudinal Plasmon band, nm	Absorbance value at the peak maximum
Citrate	550	1.5	-	-
CTAB	530	2.25	715	2.75

As seen from Figure 17, the nanoparticles prepared with the CTAB capped gold nanoseeds show a second absorption peak at longer wavelength due to the

longitudional surface plasmon oscillation. Whereas when seeding was done with citrate capped gold nanoparticles, a spectrum (Figure 17) similar to the plasmon absorption spectrum of pure seeds (Figure 16) was observed. Therefore it was decided that CTAB capped gold seeds result in gold nanorods with single crystalline structure unlike citrate capped gold seeds and thus they were utilized to produce gold nanorods through out this study.

3.1.3.2 Optimization of CTAB concentration

Surfactant used in the seed and growth solutions is composed of trimethyl ammonium bromide head group and an alkyl chain shown in Figure 6. The general trend is that, as the length of the alkyl chain is increased; higher-aspect ratio nanorods can be obtained (Nikoobakht & El-Sayed, 2003). Therefore, in our studies the surfactant having the largest carbon number, cetyltrimethylammonium bromide (C_{16}TAB) was used as a stabilizing agent and a directing agent for gold nanorod synthesis.

The effect of CTAB concentration on the aspect ratio of the nanorods formed was examined by altering the molarity of CTAB from 0.05 M to 0.15 M. The surface plasmon absorption spectra of the formed particles are presented in the Figure 18. The wavelengths of the longitudional and transverse plasmon bands at their maximum and the corresponding absorbance values are given in Table 2.

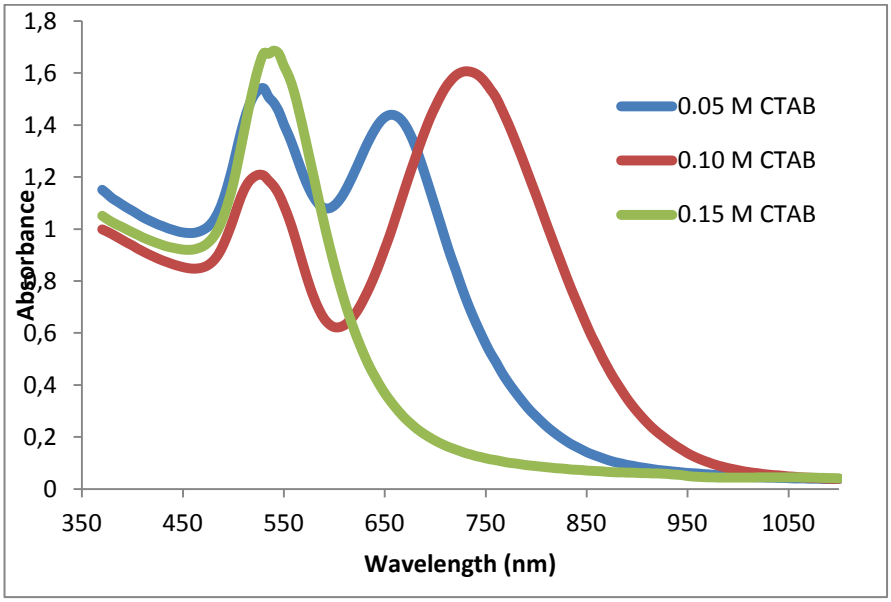

Figure 18 UV-visible absorption profile of gold nanorod solutions which prepared by varied concentration of surfactant CTAB.

Table 2 The plasmon bands of gold nanorod solution prepared by varied concentration of surfactant CTAB and with 0.50 mM $HAuCl_4$, 0.10 mM $AgNO_3$, 1.0 mM ascorbic acid and 6 µL of CTAB capped gold seed solution.

Concentration of Surfactant CTAB (M)	Peak maximum of Transverse Plasmon band, nm	Absorbance value at the peak maximum	Peak maximum of Longitudinal Plasmon band, nm	Absorbance value at the peak maximum
0.05	535	1.6	660	1.4
0.10	530	1.2	745	1.6
0.15	545	1.8	-	-

Growth solution which has 0.10 M CTAB gave the maximum redshift in the plasmon absorption. As shown in Figure 18 and listed in Table 2 longitudional surface plasmon peak is formed at 745 nm and its peak height is higher than that of the transverse surface plasmon peak. These observations are all pointing out larger aspect ratio nanorod formation. Low concentration of CTAB on the other hand,

results in the formation of short nanorods or spheroids. As seen from the Figure, longitudional surface plasmon peak of nanorods prepared with 0.05 M CTAB is lower than their transverse surface plasmon peak and their longitudinal plasmon band maximum appears at 660 nm which shows the aspect ratio of gold nanorods less than 2. The concentration of CTAB was quite critical. As shown in Figure 18, when its concentration was rised further to 0.15 M, only one surface plasmon peak indicating spherical nanoparticle formation was appeared at 530 nm i.e growth solution containing 0.15 M CTAB could not direct the nanorod formation. Therefore 0.10 M CTAB concentration was decided to be used in the growth solution.

3.1.3.3 Optimization of Silver Nitrate Concentration in Growth Solution

Absorption spectrum of the growth solution containing silver ions was taken and the silver plasmon band at 400 nm was not observed. This was an expected result. Because ascorbic acid is a weak reducing agent and silver ions could be reduced by ascorbic acid unless the pH of the solution is above 8. Thus, silver should be in the ionic form in the growth solution and as stated by Jana et al. (2001), probably, Ag^+ ion forms silver bromide on the gold particle surface and restricts growth to stabilize the rods

The effect of $AgNO_3$ concentration on the aspect ratio of the nanorods formed was examined by altering the volume of 10 mM $AgNO_3$ from 0 μL to 250 μL. The plasmon absorption spectra of the formed particles are presented in the Figure 19 and Figure 20. The wavelengths of the longitudional and transverse plasmon bands at their maximum and the corresponding absorbance values are given in Table 3.

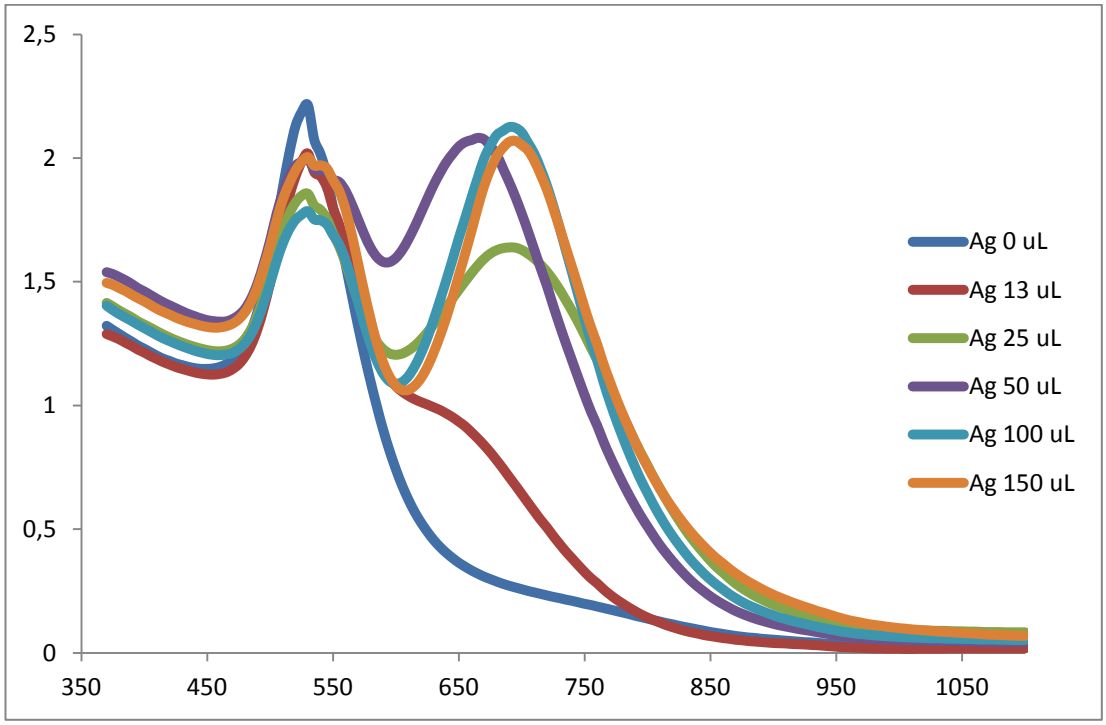

Figure 19 UV-visible absorption profile of gold nanorod solutions which prepared by varied volume of 10 mM silver nitrate (0-150 µL).

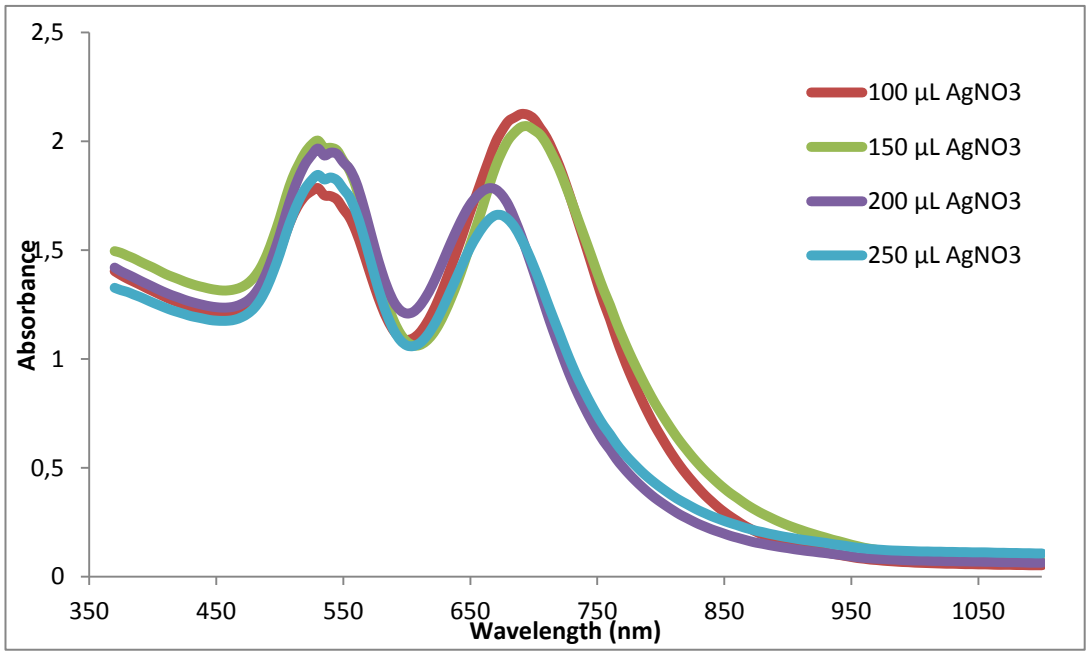

Figure 20 UV-visible absorption profile of gold nanorod solutions which prepared by varied volume of 10 mM silver nitrate (100-250 µL).

Table 3 The plasmon bands of gold nanorod solution prepared by varied volume of 10 mM $AgNO_3$ and with 4.75 mL 0.10 M CTAB, 0.50 mM $HAuCl_4$, 1.0 mM ascorbic acid and 6 μL of CTAB capped gold seed solution.

Volume of Silver Nitrate (μL)	Peak maximum of Transverse Plasmon band, nm	Absorbance value at the peak maximum	Peak maximum of Longitudinal Plasmon band, nm	Absorbance value at the peak maximum
0	535	2.20	-	-
13	535	2.05	-	-
25	535	1.85	700	1.63
50	535	1.95	660	2.07
100	535	1.70	695	2.12
150	535	1.95	700	2.05
200	535	1.95	670	1.78
250	540	1.83	680	1.64

As shown in Figure 19 and Table 3, varied volume of silver nitrate added to the growth solution in the range of 13-150 μL result in first the appearence of longitudional surface plasmon band while transverse surface plasmon band decreasing and also shifting the maximum of the longitudinal plasmon band to longer wavelengths. As noticed after the addition of 150 μL of silver nitrate no change in the plasmon absorption peak was observed. However, further increase in the concentration of silver nitrate (after addition of 200 and 250 μL of $AgNO_3$) resulted in decrease both in longitudional and transverse surface plasmon absorption peaks, Figure 20 and Table 4. These results showed us that silver nitrate concentration with a limited range helps to produce gold nanorods with higher aspect ratio. On the other hand, high concentration of silver nitrate causes a decrease in the aspect ratio of gold nanorods. Nikoobakht & El-Sayed (2003) stated that the reason of the blueshift in the

wavelength of the longitudinal plasmon band is due to the increase in ionic strength of the medium.Therefore we decided to keep the silver nitrate concentration in the range of 0.10-0.30 mM in the final solution. As a result of this, gold /silver salt ratio is in the range of 1.5 and 5.0.

3.1.3.4 Optimization of Ascorbic Acid Concentration in Growth Solution

The mild reducing agent, ascorbic acid has a crucial role to produce homogeneous gold nanorods in various morphologies, Figure 20 shows the reduced and oxidized forms of ascorbic acid.

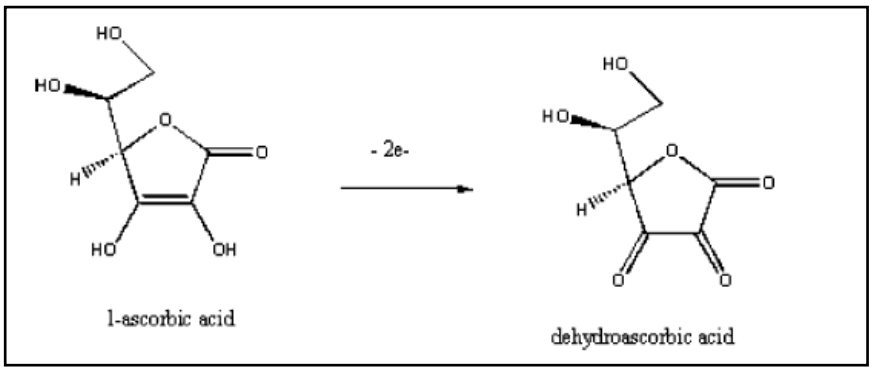

Figure 21 Schematic representation of reduction of ascorbic acid to diascorbate anion (Wikimedia Foundation, Inc., 2011).

Ascorbic acid gives two electrons and gold ions receive three electrons. Therefore stochiometrically, ascorbic acid concentration corresponding 3:2 the concentration of the gold ions in the growth solution should be enough for a complete reduction (Miranda, Dollahon, & Ahmadi, 2006).

Au^{+3} ions are reduced to Au^{+} by using ascorbic acid and the concentration of ascorbic acid determines the number of reduced gold atom. Reducing power of ascorbic acid is not enough to reduce gold ions to zerovalent state. Metallic gold formation takes place in a reaction medium through underpotential deposition on the

gold nanoseeds. The reducing power of ascorbic acid is not also enough to reduce silver ions in the reaction medium due to low pH value of solution.

The effect of ascorbic acid concentration on the aspect ratio of the nanorods formed was examined by altering the volume of 0.10 M ascorbic acid from 30 µL to 55 µL. The plasmon absorption spectra of the formed particles are presented in Figure 22. The wavelengths of the longitudional and transverse plasmon bands at their maximum and the corresponding absorbance values are given in Table 4.

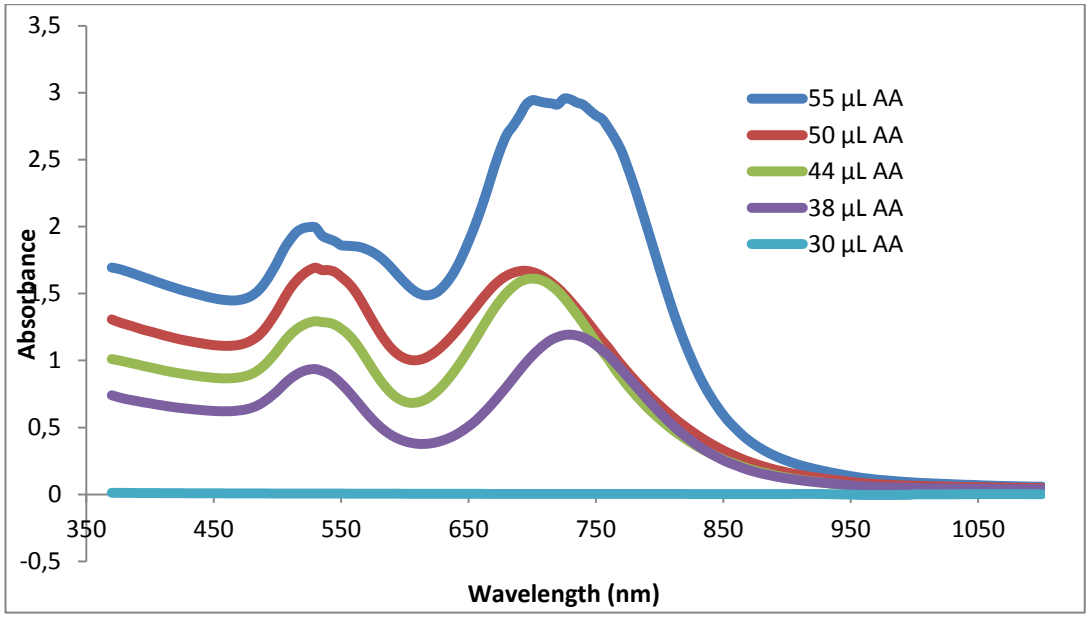

Figure 22 UV-visible absorption profile of gold nanorod solutions which prepared by varied volume of 0.10 M ascorbic acid (AA) (30-55 µL).

Table 4 The plasmon bands of gold nanorod solution prepared by varied volume of 0. 10 M Ascorbic acid with 4.75 mL 0.10 M CTAB, 0.50 mM $HAuCl_4$, 0.10 mM $AgNO_3$, 1.0 mM ascorbic acid and 6 μL of CTAB capped gold seed solution.

Volume of Ascorbic Acid (μL)	**Peak maximum of Transverse Plasmon band, nm**	**Absorbance value at the peak maximum**	**Peak maximum of Longitudinal Plasmon band, nm**	**Absorbance value at the peak maximum**
30	-	-	-	-
38	540	0.82	760	1.17
44	545	1.24	705	1.61
50	540	1.66	700	1.61
55	540	1.91	720	2.91

As can be understood both from Figure 22 and Table 4, at all concentrations of ascorbic acid the longitudional and transverse plasmon bands are clearly observed except, 30 μL 0.10 M ascorbic acid solution. The maximum red shift in the position of the longitudional plasmon band was obtained with a growth solution containing 55 μL of 0.10 M ascorbic acid. This was the highest concentration of ascorbic acid used in our gold nanorod preparation experiments. It was stated that (Gou & Murphy, 2005), the morphology of gold nanorods converted to dogbone shape by increasing the amount of ascorbic acid. They claim that high concentration of ascorbic acid fastly reduces gold ions while rod formation is taking place slowly. Thus the accumulation of the excess gold metal at the edges causes an increase in size at the tips of gold nanorods.

The morphology of the prepared nanorods was examined. HR-TEM images of gold nanorods synthesized with different volume of 0.10 M Ascorbic acid are given in Figure 23.

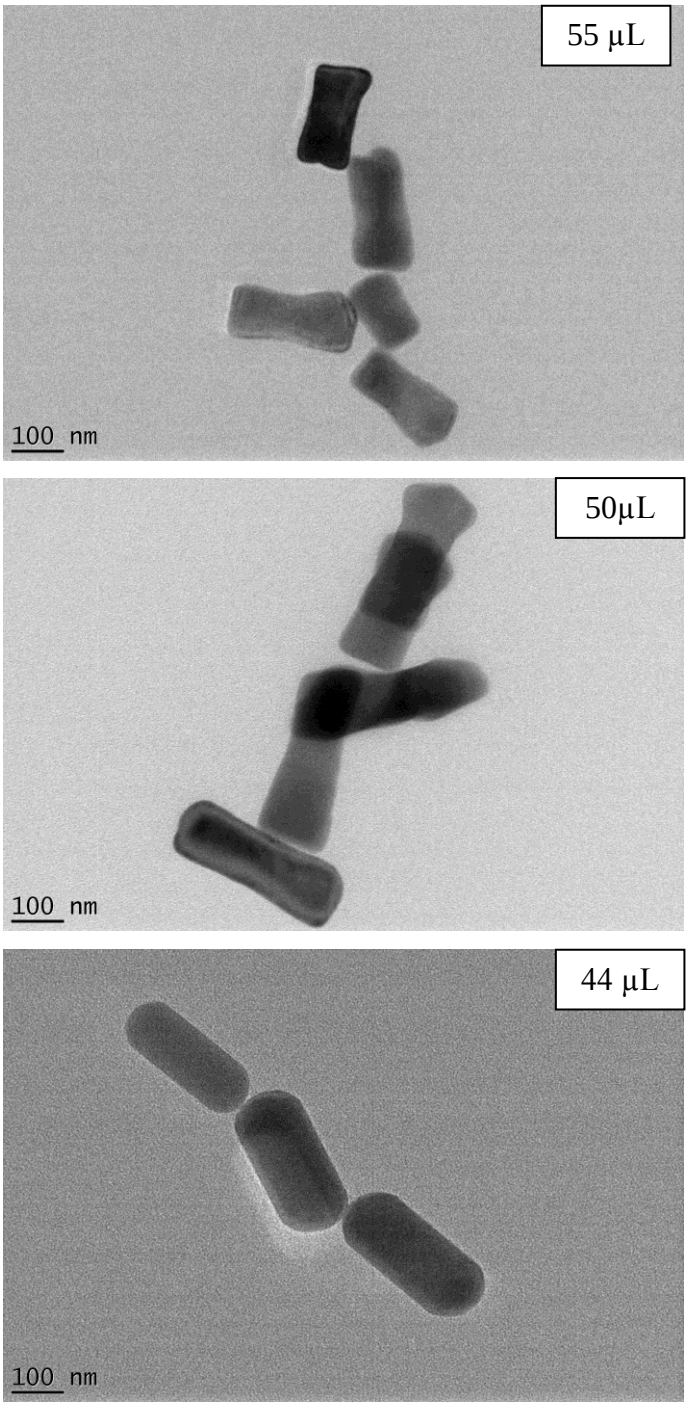

Figure 23 HR-TEM images of gold nanorods synthesized with different volume of 0.10 M Ascorbic acid. Inset a) 55 µL b) 50 µL and c) 44 µL.

As can be seen from Figure 23, dog bone shape formation starts to appear when 50 µL of 0.10 M ascorbic acid is used. Therefore, in our studies concentration of

ascorbic acid was set to 44 µL in order to obtain homogeneous gold nanorods instead of dogbone shaped ones.

3.1.3.5 Optimization of Volume of Seed Solution Added to Growth Solution

As mentioned in section 3.1.3.4 catalytic reduction of gold ion to metallic gold takes place only on the surface of gold seeds introduced into the growth solution. Therefore the number of nucleation centers has a direct relationship with the number of synthesized gold nanorods and their aspect ratios.

The effect of added gold seed solution concentration on the aspect ratio of the nanorods formed was examined by altering the volume of seed solution from 3.0 µL to 12.0 µL. The plasmon absorption spectra of the formed particles are presented in Figure 24. The wavelengths of the longitudional and transverse plasmon bands at their maximum and the corresponding absorbance values are given in Table 5.

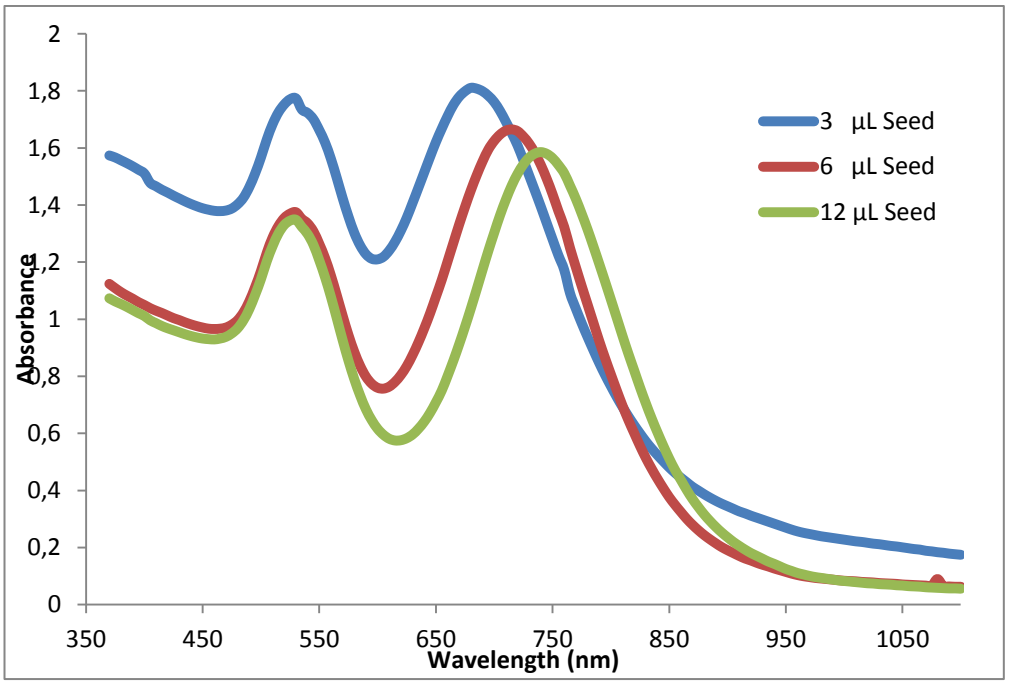

Figure 24 UV-visible absorption profile of gold nanorod solutions which prepared by varied volume of CTAB stabilized seeds.

Table 5 The plasmon bands of gold nanorod solution prepared by varied volume of CTAB stabilized gold seeds and with 0.50 mM $HAuCl_4$, 0.10 M CTAB, 0.10 mM $AgNO_3$, and 1.0 mM ascorbic acid.

Volume of CTAB Stabilized Seed Solution (μL)	**Peak maximum of Transverse Plasmon band, nm**	**Absorbance value at the peak maximum**	**Peak maximum of Longitudinal Plasmon band, nm**	**Absorbance value at the peak maximum**
3	530	1.8	690	1.8
6	530	1.4	725	1.6
12	530	1.4	745	1.5

As shown in the Figure 24, increasing concentration of gold seed has a red shift in the the longitudional surface plasmon band of the gold nanorods due to the increase in the aspect ratio of gold nanorods.vFor homogeneous gold nanorod production, parameters that affect the morphology of gold nanorods were set as shown in Table 6.

Table 6 Optimum Growth Conditions for Gold Nanorod Production

Parameters (μL)	
0.1 M CTAB	$4.75x10^3$
0.01 M $HAuCl_4$	250
0.01 M $AgNO_3$	50
0.1 M Ascorbic Acid	44
Gold Seed Soln.	6

3.1.4 Gold-Silver Core-Shell Nanorods

SERS enhancement effect of silver is higher than gold in the VIS region of the spectrum. Silver nanorod synthesis studies in our group have started with Rukiye Sancı and continued with Lütfiye. S. Keser. In the former study, few nanorods with large number of spheroids, whereas in the latter case high yield of uniform size silver nanorods mixed with silver nanoparticles had been obtained.

Therefore, once we have established the preparation of homogeneous gold nanorods we decided to use them as platforms to produce gold core silver shell nanorods. Besides, core-shell bimetallic morphology of gold nanorods covered with silver has dual character and they might have three different surface plasmon peaks with respect to silver shell thickness.

The effect of silver nitrate concentration on the aspect ratio of the nanorods formed was examined by altering the volume of 1 mM silver nitrate from 0 µL to 900 µL. The plasmon absorption spectra of the formed particles are presented in Figure 25.

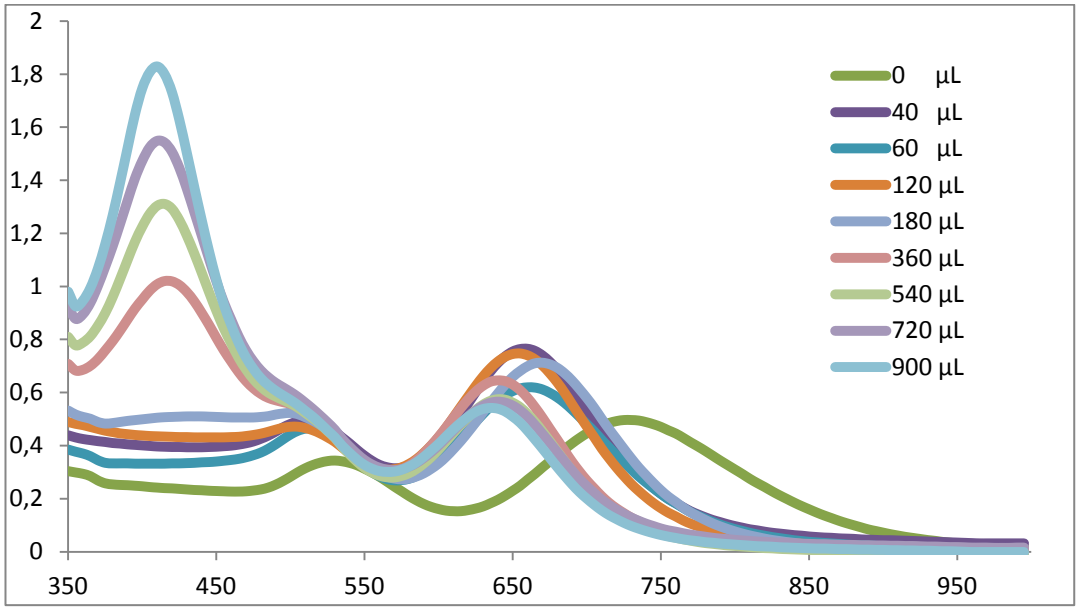

Figure 25 UV-visible absorption profile of gold silver core shell nanorod solutions which prepared by varied volume of 1.0 mM $AgNO_3$.

As shown in Figure 25, surface plasmon absorption peak was grown at 400 nm as silver thickness increased. On the other hand, longitudional surface plasmon absorption band of gold nanorod was blue shifted. Increasing silver shell also increases width of rods and this causes a decrease in the aspect ratio of nanorods.

FE-SEM image and EDX pattern of the gold silver core shell nanorods synthesized with 540 μL volume of 1mM $AgNO_3$ are given in Figure 26 and Figure 27 respectively.

Although the SEM image is not informative in terms of morphologies of the particles, the presence of Ag on the gold nanorods is investigated by the EDX spectrum.

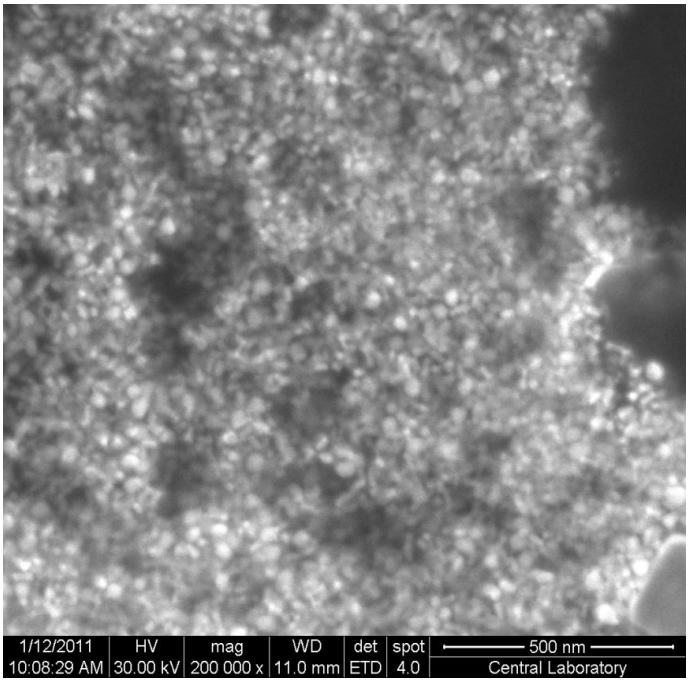

Figure 26 FE-SEM images of gold silver core shell nanorods.

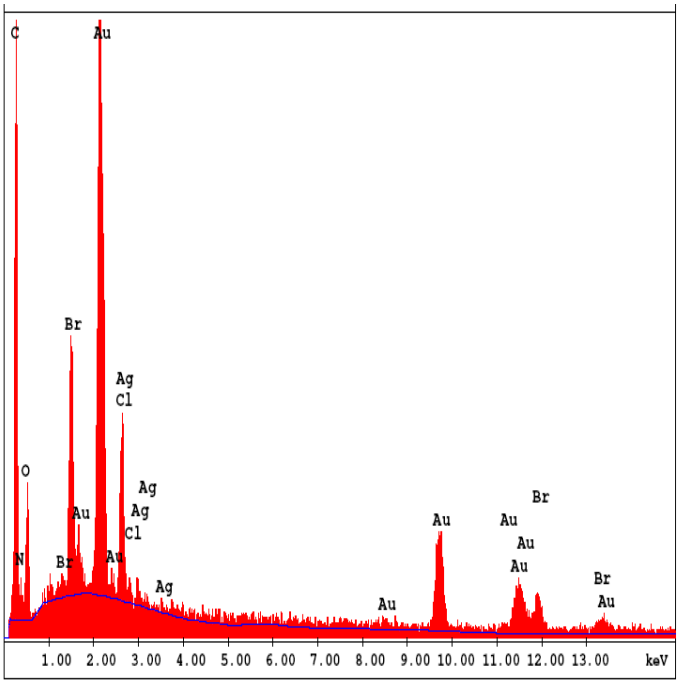

Figure 27 EDX patterns of the gold silver core shell nanorods.

3.2 Nanoconjugation

L-Cysteine is used as a linker molecule in this study to prepare aggregates of gold nanorods and nanospheres and silver nanospheres. The surface plasmon absorption and electromagnetic enhancement properties of these aggregates were investigated.

3.3 End-to-End Self Assembly of Gold Nanorods and Gold Nanospheres by Using L-Cysteine

As mention previously, CTAB double layers at the end points of gold nanorods are not very stable compared to the ones at the sites. Cysteine molecules are preferentially adsorbed at the ends of the gold nanorod particles and their interaction with each other form chain like assembly as shown in Figure 28.

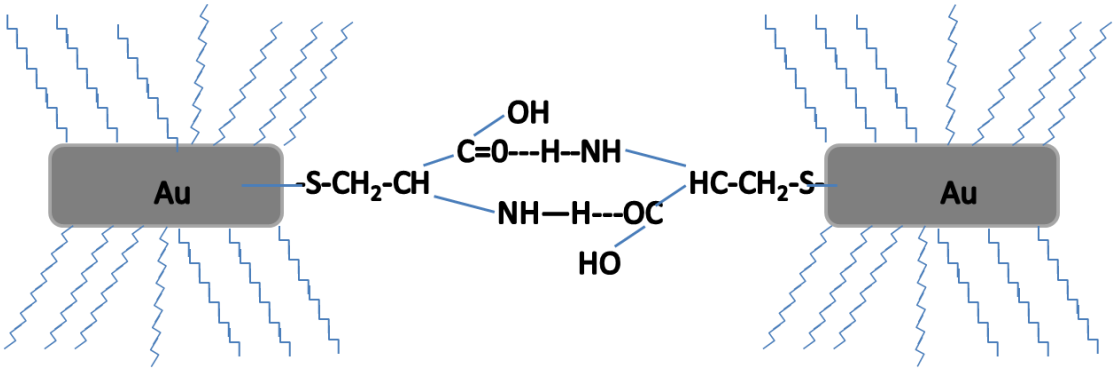

Figure 28 Thiol groups of cysteine molecules attached to the tip points of gold nanorods.

According to Hu et al. (2005), end to end assemblies of gold nanorods occur with hydrogen bonding between carboxyl and amine groups as shown in Figure 28. On the other hand, Sun et al. (2008) claimed that assembly occurred with electrostatic interaction (Sudeep, Joseph, & Thomas, 2005; Hu, Cheng, Wang, Wang, & Dong, 2005; Zhang, et al., 2007).

The pKa values of cysteine are 1.92 and 10.70. Below the second pKa value of cysteine, amine groups are positively charged and carboxylate groups are negatively charged, Figure 29.

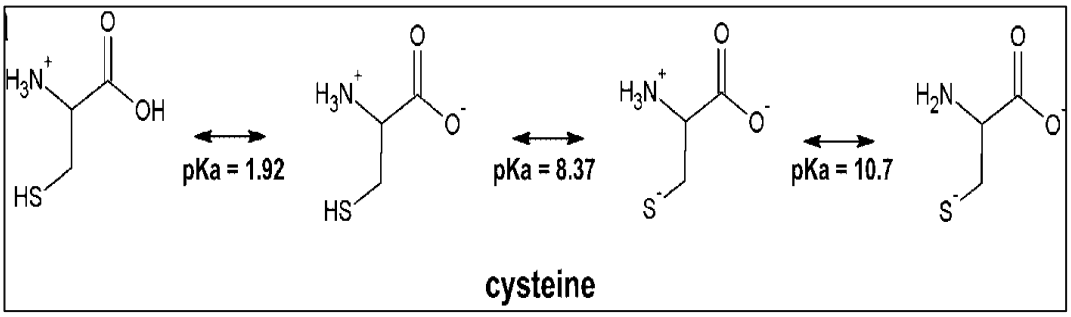

Figure 29 pKa values of Cysteine molecule.

pH dependent assembly of gold nanorods was examined by altering the pH value of gold nanorod solution from 6.35 to 2.13. The plasmon absorption spectra of the assembled particles are presented in Figure 30.

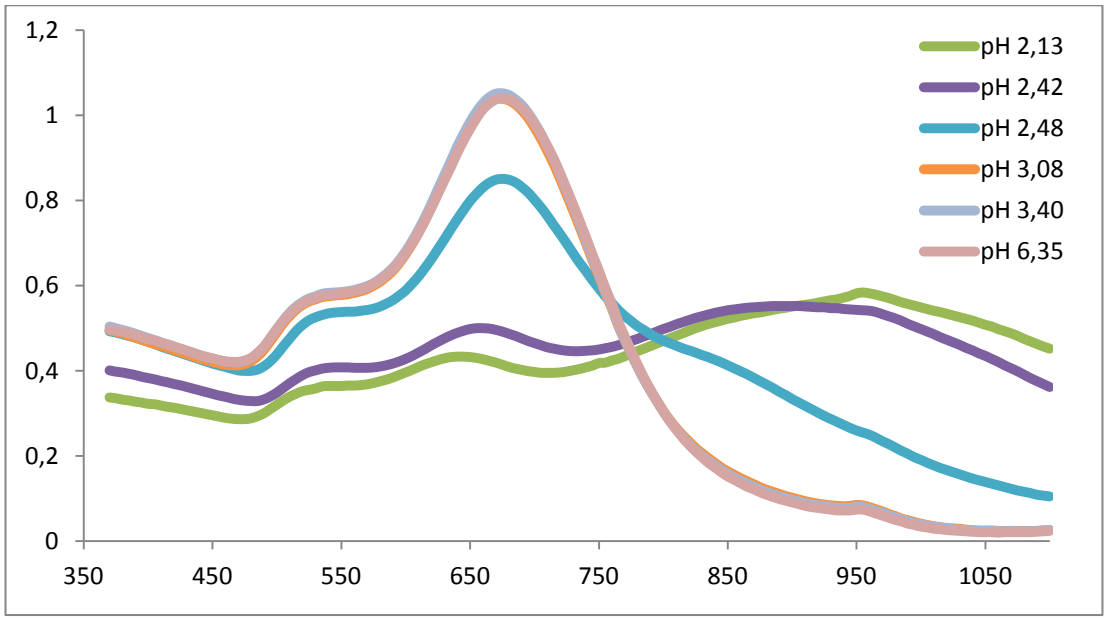

Figure 30 UV-visible absorption profile of pH dependent end to end self assembled gold nanorods with linker molecule Cysteine.

Cysteine molecule should be in zwitterionic form when pH value is kept in the range of roughly 2.00 to 8.00. At this pH range, electrostatic interactions between oppositely charged groups of cysteine on the neighboring gold nanorod tips should result in assembly. However as shown in Figure 31, the maximum plasmon band shift to longer wavelength occurs at pH values of 2.42 and 2.13. Hence it was concluded that the chain formation of gold nanorods by using cysteine as linker molecules occur below pH 3.50.

Self assembly of gold nanorods is time dependent and examined by UV-vis spectroscopy. Shifth in the plasmon absorption spectra of the assembled particles are presented in Figure 31.

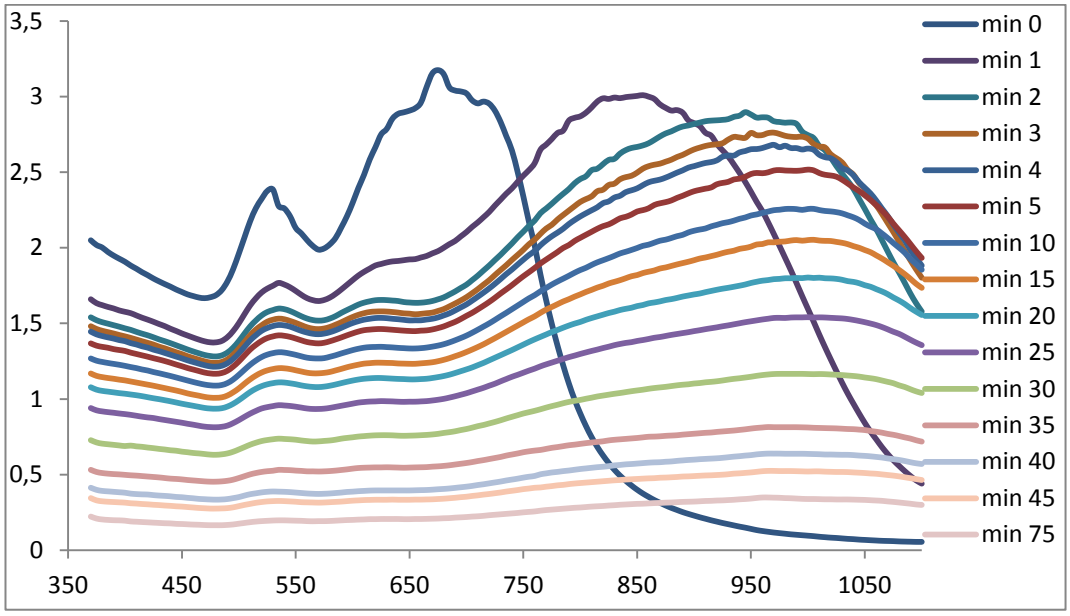

Figure 31 UV-visible absorption profile of time dependent end to end self assembled gold nanorods with linker molecule Cysteine. (0.10 mM Cys, pH: 2,20, Temp: 25 ^{o}C)

As a result of this time dependent change, longitudional surface plasmon peak of monodisperse gold nanorods lessened and longitudional surface plasmon peak of assembled gold nanorods get stronger with time (0-75 min). In 40 minutes, almost all gold nanorods take place in chain formation and longitudional surface plasmon band redshifted from 700 nm to 1050 nm region as shown in Figure 31.

Assembly of gold nanorods is a kinetically controlled process. Thus the parameters like the concentration of cysteine and gold nanorods, temperature should also be determining factors in the rate of the chain formation process. Therefore the discussion given above is valid only at the specified conditions.

The TEM images of the prepared gold nanorod chains at the specified conditions are given in Figure 32.

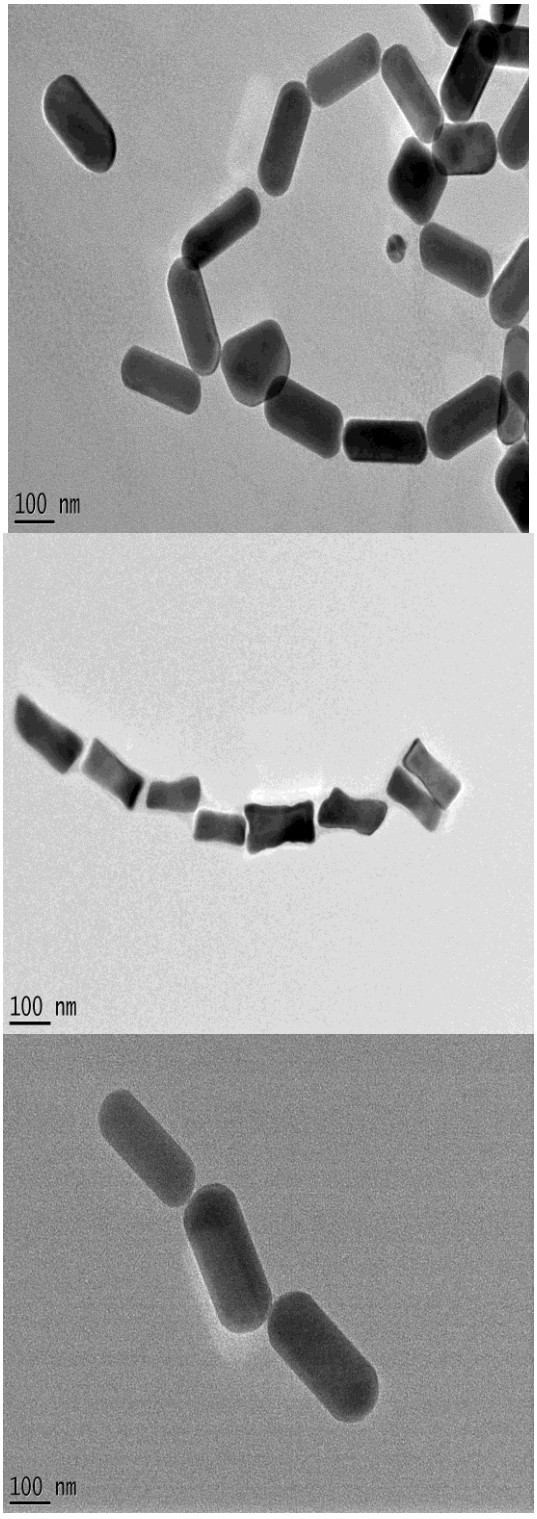

Figure 32 TEM images of end to end self assembled gold nanorods. All chain formation takes place at the conditions (0.10 mM Cys, pH: 2,20, Temp: 25 ^{o}C).

The formation of homogeneous and dogbone type nanorod chains after the addition of cysteine are evidenced in the TEM images shown in Fig. 32.

Spherical gold nanoparticles form aggregates instead of chain formation. The effect of pH and duration of the reaction between gold nanoparticle and cysteine to the gold nanoparticle aggregate formation were investigated by UV-vis spectrophotometry. The results are presented in Figure 33 and Figure 34.

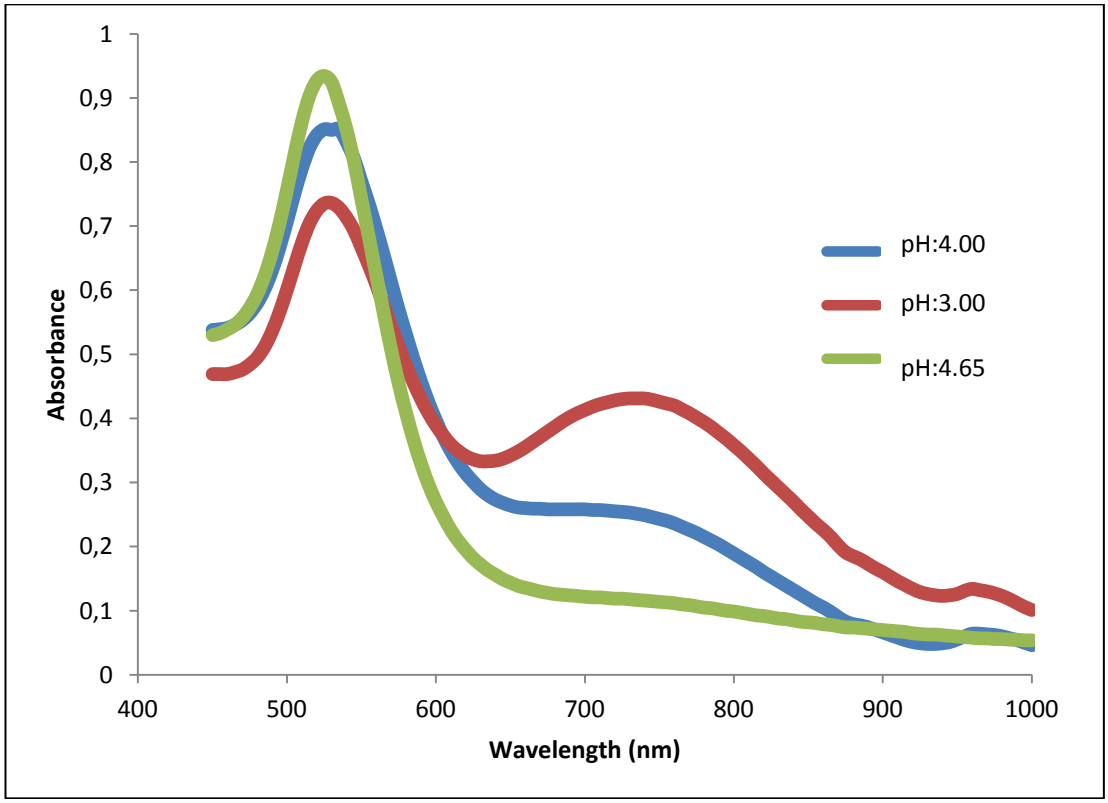

Figure 33 UV-Vis absorption spectra of gold nanoparticles in the presence of 1.0 x10^{-6} M Cysteine at different pH values.

As seen from spectra in Figure 33, among the pH values examined, pH: 3.00 was chosen as the most appropriate one. At this pH, the peak around 520 nm due to the plasmon band of unconjugated Au nanoparticles is still exist and the plasmon peak

around 750 nm is appeared owing to agglomeration of the particles due to the presence of cysteine linker. Lower pH values caused nanoparticles to settle out quicly due to excessive agglomerate formation. As can also be seen from Figure 34, even at pH 3.00, the intensity of the red shifted peak is decreased as time passes due to the precipitation of the nanoparticles-cysteine agglomerates. Therefore it is better to take the measurements in a short time period.

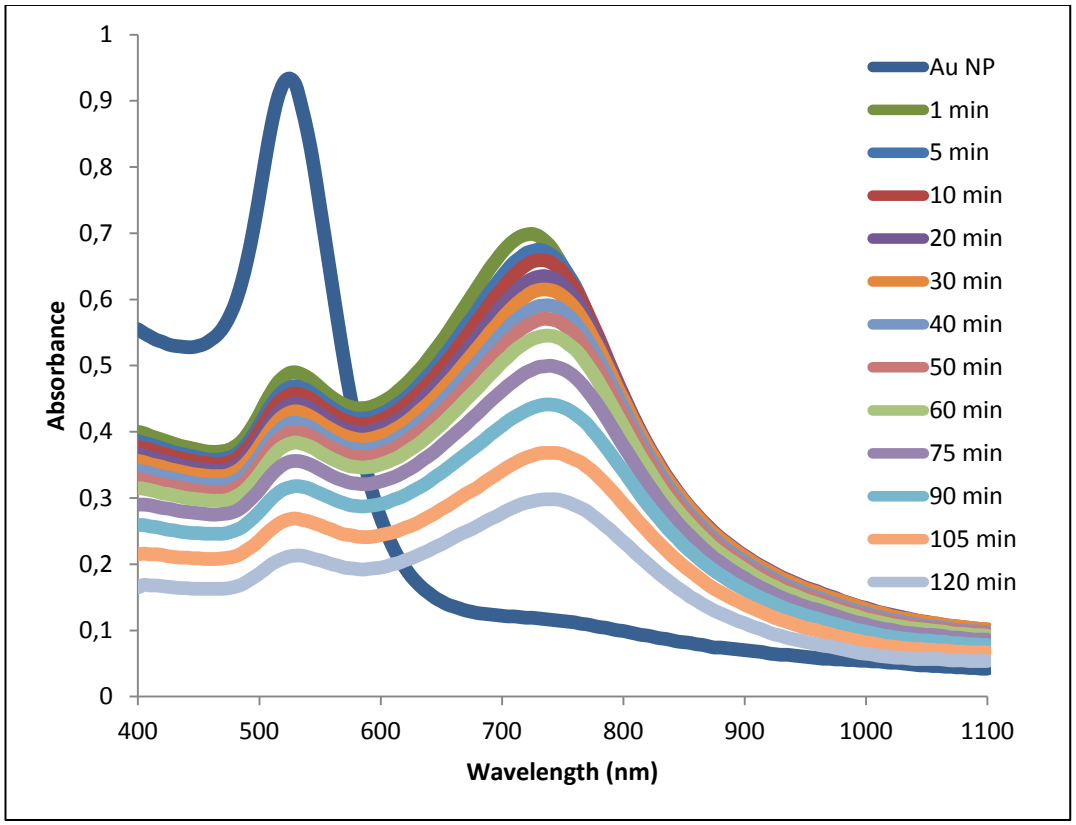

Figure 34 Time dependent absorption spectra of gold nanoparticles (pH: 3.00) with $5.0x10^{-6}$ M Cysteine.

3.4 Detection of Cysteine with different Nanostructures

In this section the electromagnetic enhancement performances of gold nanoparticles, silver nanoparticles, gold nanorods and gold silver core shell nanorods will be investigated for the determination of cysteine by SERS. The normal Raman spectrum of solid cysteine is depicted in Figure 35. Cysteine molecule has three different

functional groups which are thiol, amine and carboxyl groups. Among these groups, thiol group has the highest streching and bending vibrations with respect to other groups. Therefore, in this section, only C-S bond vibrations will be followed. Detailed SERS analysis of cysteine is given in section 3.5.2. As discussed in the previous section, sulfur atom of cysteine molecule is attached to end points of gold nanorods and form nanorod chains. On the other hand, sulfur atoms are attached to whole surface of citrate stabilized spherical gold nanoparticles and form nanoclusters instead of chains. Electromagnetic enhancement among nanostructures increases as the gap between particles decreases. Therefore, the SERS enhancement of Cysteine molecule between two neighboring metal nanorods or in a gold nanoparticle cluster is expected to be more pronounced. Here, we have to point out that we are working at the VIS region of the spectrum where silver is better scatterer than gold whereas in the NIR region just the opposite is true.

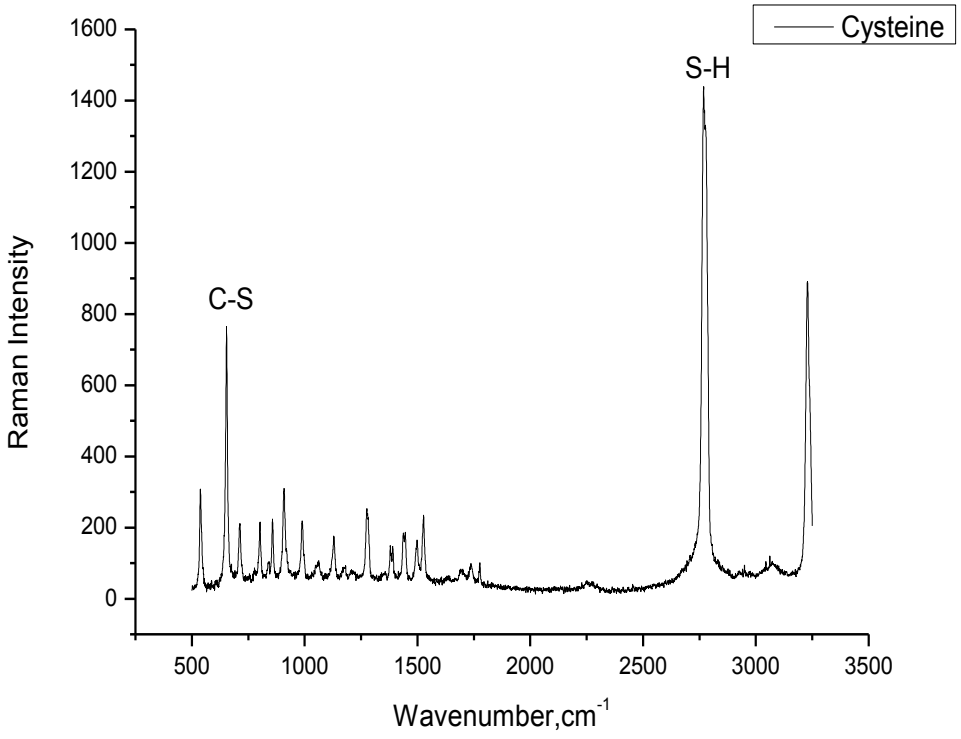

Figure 35 Raman spectrum of solid Cysteine.

For SERS studies, prepared nanostructures were mixed with cysteine solution in the acidic medium (pH: 2.20). SERS spectra of the cysteine were acquired in 20 s. data acquisition times. As shown in Figure 36, C-S bond stretching at 668 cm^{-1} were observed for three different substrates.

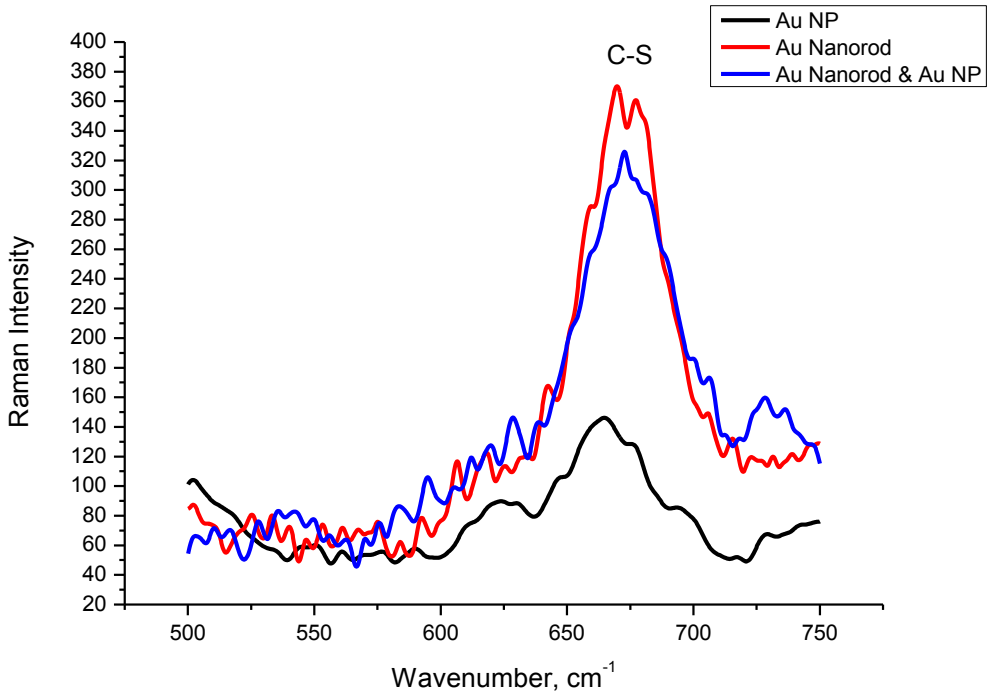

Figure 36 SERS Spectrum of $1x10^{-4}$ M Cysteine with different nanostructures (pH: 3.00).

As can be seen from Figure 36, the intensity of the peak obtained with gold nanorods is higher than that of gold nanospheres. Because, original nanoparticle solutions were used without any dilution or concentration process. Gold salt concentration used in gold nanorod production was approximately 20 times more than that of gold nanosphere synthesis. Therefore, the gold nanorod solution is more concentrated than nanosphere solution.

SERS spectra of 0.10 mM Cysteine with silver nanoparticles and gold-silver core shell nanorods are shown in Figure 37.

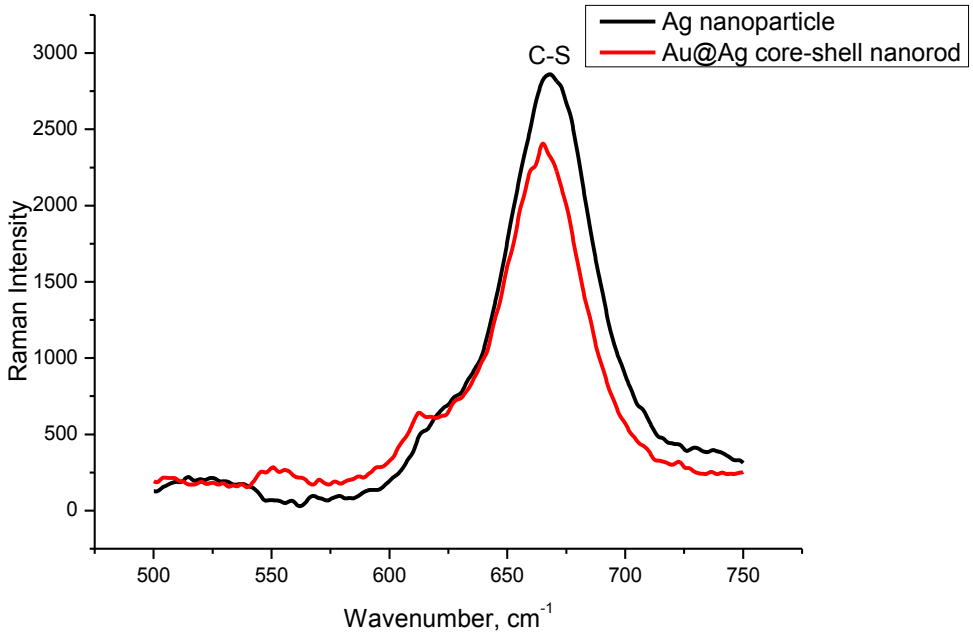

Figure 37 SERS Spectrum of $1x10^{-4}$ M Cysteine with different nanostructures (pH: 3.00).

As can be seen from the Figure 37, the enhancement properties of core shell gold silver nanorods and silver nanoparticles are almost the same.

We can conclude that all these prepared nanostructures can be used as a proper SERS substrate.

3.5 Determination of Cysteine

3.5.1 Colorometric Determination of Cysteine

UV-vis absorption of directed self-assembly of gold nanoparticles had been employed to the highly specific chemical recognition of oligonucleotide base-pairing

between complementary chains in our laboratory by Seher Karabıçak. In her thesis hybridization of complementary DNA strands capped with thiols were attached to two batches of colloidal gold nanoparticles. Mixing of these two solutions resulted in the formation oligonucleotide duplex in between gold nanoparticles and caused them to aggregate. By monitoring the collective surface plasmon resonance of the assembly or the color of the mixture solution hybridization was investigated. This time UV-vis absorption of directed self-assembly of gold nanoparticles will be used for the colorimetric determination of cysteine.

The interaction of gold nanoparticles (rod and sphere) with cysteine is explained in section 3.4 in detail. As shown in Figure 31, the plasmon absorption bands of nanorods at around 650 nm are shifted to the 950 nm, whereas that of nanospheres were changed from 540 nm to 750 nm after the addition of cysteine due to the electric dipole–dipole interaction and coupling between the neighboring particles in the aggregates.

The wavelength change in the plasmon absorption spectra of nanosphere solution after cysteine addition occurs in the Vis region (540nm to 750 nm). Therefore it is coupled with a color change of red to purple.

In order to see the effect of cysteine concentration on aggregate formation, pH of the solution was set to 3.00 at which the associations of the nanospheres were taking place and the volume of the gold nanospheres was kept constant. Various concentration of cysteine was added to the gold nanosphere solution and the shift in the plasmon absorption band was followed spectrophotometrically (Figure 38). The color change upon cysteine addition to pH adjusted gold nanoparticles were also followed visually as can be seen from Figure 39.

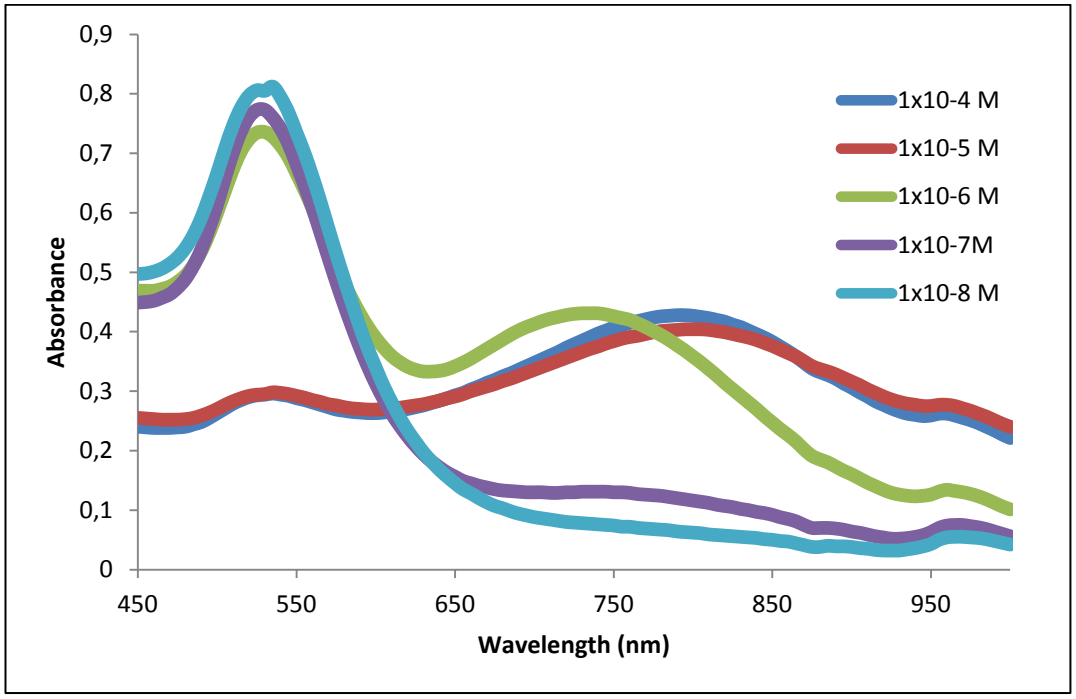

Figure 38 Absorption spectra of gold nanoparticle solutions having various concentration of Cysteine ($1x10^{-4}$ M-$1x10^{-8}$ M) at pH: 3.00.

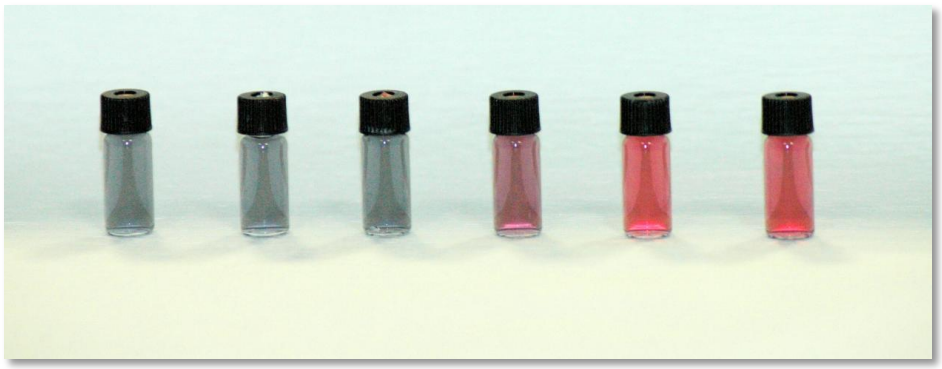

Figure 39 Cysteine added Au NP solutions (pH:3.00) (from left to right:$1.0x10^{-3}$ M, $1.0x10^{-4}$ M, $1.0x10^{-5}$ M, $1.0x10^{-6}$ M, $1.0x10^{-7}$ M and Au NP without Cys)

As can be seen from Figure 38, the second Plasmon peak at longer wavelength is started to appear slightly when cysteine concentration becomes $1.0x10^{-7}$ M. The intensity of the Plasmon band is increased parallel to an increase in cysteine concentration to $1.0x10^{-6}$ M indicating an increased extent of nanoparticle assembly.

Further increase in cysteine concentration causes a constant red shift in Plasmon bands without any change in their intensities.

The visual inspection of these samples shows that gold nanoparticle solution containing $1.0x10^{-6}$ M cysteine appear to be purple and solutions without gold-cysteine assembly formation are red.

Both spectrophotometric measurements and visual inspection, point out almost the same minimum cysteine concentration, $1.0x10^{-6}$ M, for the detectable gold nanoparticle-cysteine interaction/ assembly formation. In other words, $5.0x10^{-6}$ M is the lowest cysteine concentration detected by this colorimetric method. Our result is consistent with the literature (Rusin O. , et al., 2004).

The detection strategy for cysteine based on the color change originated from the cysteine-directed self-assembly of gold nanoparticles is a rapid and simple procedure and if visual examination is preferred, it does not need any instrumentation at all. However, there are some disadvantages of this approache: a) low sensitivity, in which only micromolar concentrations of cysteine is detectable, b) it does not provide the exact concentration of cysteine, it is utilized only to understand whether the concentration of cysteine is above or below $1.0x10^{-6}$ M.

3.5.2 SERS Determination of Cysteine

In this section we will report for the first time, the quantitative determination of cysteine using SERS technique. As shown in the previous sections, in the presence of cysteine, gold nanoparticles can self-assemble to form a network structure. The large size of the assemblies of gold nanoparticles and the surface plasmon coupling among gold nanoparticles lead to strong resonance light scattering signals. This enhanced plasmon intensity is proportional to the cysteine concentration.

The SERS spectrum of $5.0x10^{-5}$ M L-cysteine is shown in Figure 40 and the frequencies corresponding to detected peaks in this spectrum are shown in Table 7.

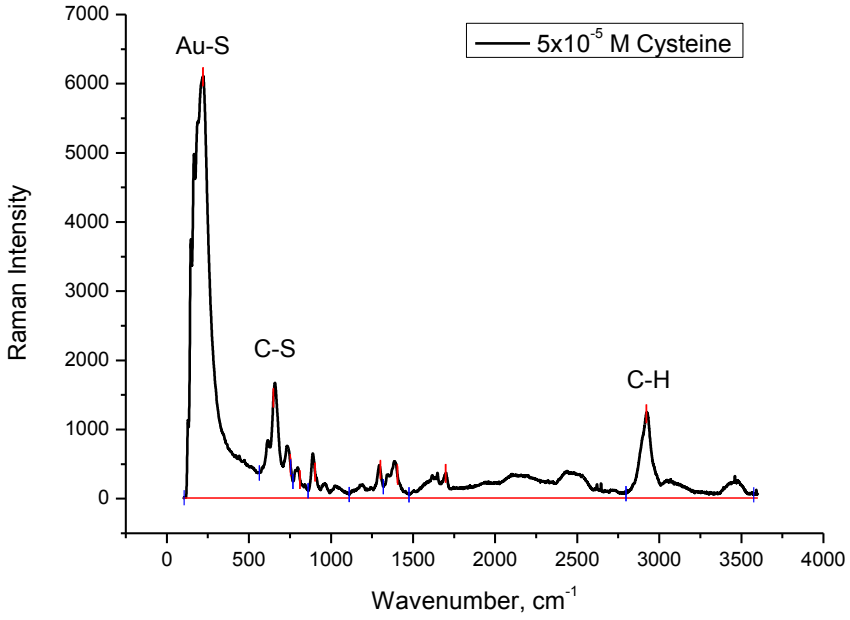

Figure 40 SERS spectrum of L-cysteine ($5x10^{-5}$M) (Au NP pH=3)

Table 7 Raman frequencies of L-cysteine and their assignment

Frequency (cm^{-1})	**Band Assignment**
221	Au-S stretching
668	C-S stretching
*2682	S-H stretching
2922	C-H stretching

*S-H band stretching which is existent in ordinary Raman cysteine spectrum, was not detected in SERS Spectrum of $5.0x10^{-5}$M Cys solution in which Au NP pH=3.00.

If the Raman spectrum of cysteine (Figure 35) is compared with the SERS spectrum of gold nanoparticle mixed cysteine of $5.0x10^{-5}$ M final concentration, there are two important peaks to be taken into consideration, Au-S and S-H. Since cysteine is

bounded to Au nanosphere surface via sulfur, S-H bond is broken and Au-S bond is formed. Therefore Au-S stretching is present at 221 cm^{-1} and S-H stretching at 2682 cm^{-1} is missing in the spectrum of spherical Au nanoparticles spiked with $5.0x10^{-5}$ M concentration of cysteine. Monitoring the intensities of the dominant peaks namely Au-S, C-S, and C-H, the quantitative analysis was achieved. $1.0x10^{-5}$ M, $2.0x10^{-5}$ M, $3.0x10^{-5}$ M, $4.0x10^{-5}$ M, $5.0x10^{-5}$ M concentrations were used for the preparation calibration plot. The SERS spectra of this analysis are indicated in Figure 41.

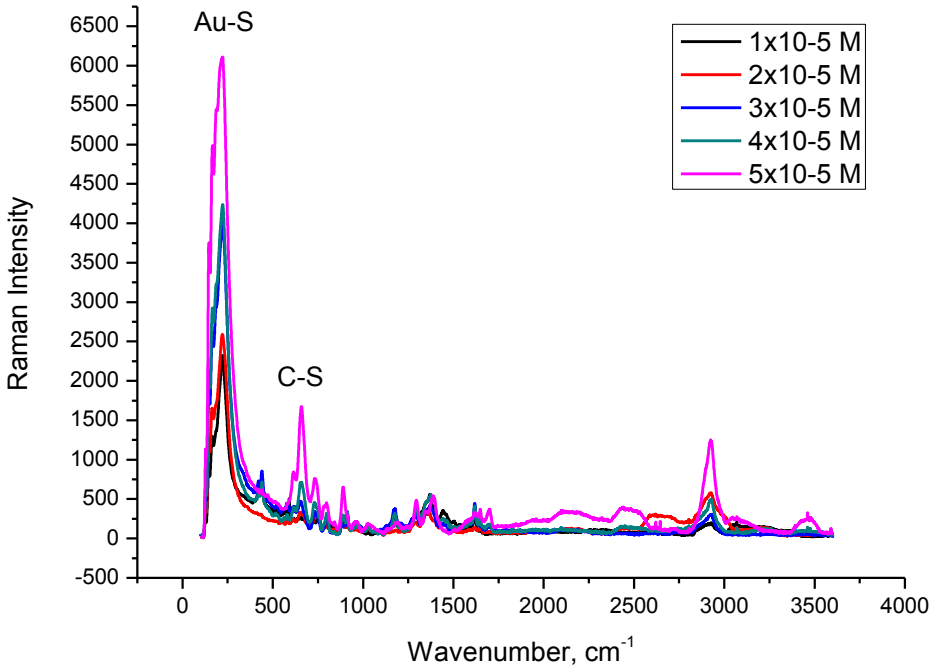

Figure 41 SERS Spectra of Cys with concentrations; $1.0x10^{-5}$ M – $5.0x10^{-5}$ M

As can be seen from the Figure 41, obtained results are consistent since the intensity of Au-S, C-S and C-H bands intensities are directly proportional with cysteine concentration, leading to quantification. Calibration plots corresponding to each of these three bands are drawn and they are shown in Figure 42, 43 and 44 respectively.

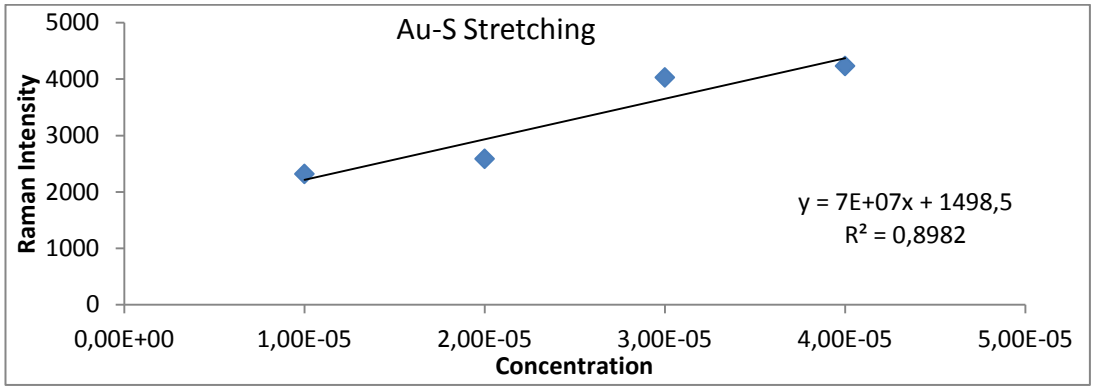

Figure 42 Calibration plot of Au- S stretching

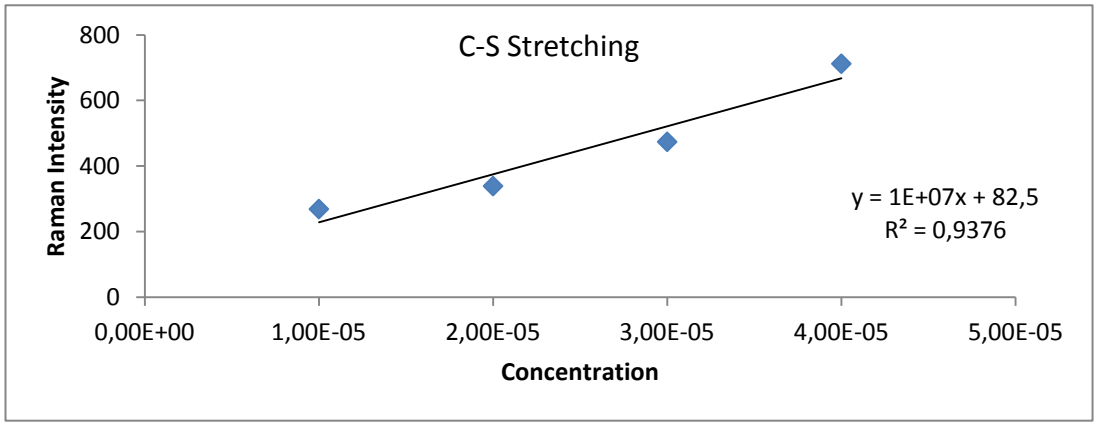

Figure 43 Calibration plot of C-S stretching

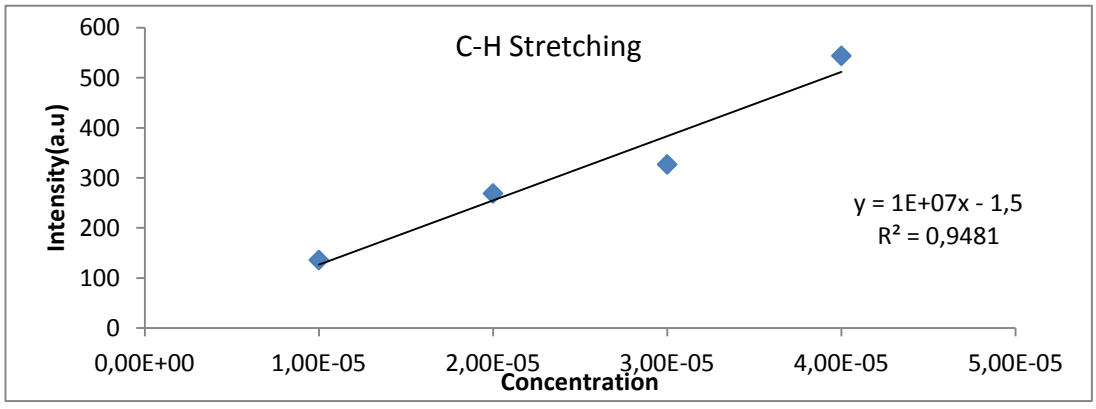

Figure 44 Calibration plot of C-H stretching

There is a good linear relationship between the SERS intensity and the concentration of cysteine in the range of $1.0x10^{-5}$ M – $5.0x10^{-5}$ M. The regression equations are given in the calibration plots, Figures 42-44. The corresponding regression coefficients are around 0.91.The relative standard deviation of 10 measurements of $1.0x10^{-5}$ M cysteine is 14%. Accordingly, as low as $1.0x10^{-6}$ M of the cysteine can be detected with the proposed method.

CHAPTER 4

4. CONCLUSION

One of the most fascinating aspects of nanosized metal structures is their optical property that finds various technological applications. Control of the structure and thereby optical properties of gold and silver nanomaterials is especially important for SERS applications because the SERS enhancement factor depends on the optical absorption of the substrate.In this study, silver and gold nanoparticles were synthesized by citrate reduction technique, gold nanorods were prepared by silver assisted seed mediated surfactant directed growth method and core shell gold silver nanorods were produced by reduction of silver on the surface of gold nanorods. Synthesized nanostructures were characterized by UV-vis Spectroscopy, Field Emission- Scanning Electron Microscopy, Energy Dispersive X-ray analysis and High Resolution-Transition Electron Microscopy.

The electromagnetic enhancement performances of gold nanoparticles, silver nanoparticles, gold nanorods and gold silver core shell nanorods were investigated through SERS measurements by using cysteine as a model compound. The results have shown that all of the aforementioned nanostructures can be used as an efficient SERS substrate in Vis-NIR region of the EM spectrum.

Applications of metal nanoparticles to next generation scientific studies require new designs and improvements in their assembly to more complicated structures. Hence, cysteine is used as a linker molecule in this study to prepare aggregates of gold nanorods and nanospheres and silver nanospheres. The most critical parameters controlling the assembly process was the pH of the medium and cystein concentration. In order to establish the strongest electrostatic interaction between

cysteine molecules, the pH of the system should be around 3.00. A cystein concentration of 1.0x 10^{-6} M was required for the visual detection of cluster formation. The surface plasmon absorption and electromagnetic enhancement properties of these aggregates were also investigated.

Cysteine is an important amino acid. The defficiency of cysteine can cause slow growth, hair depigmentation, edema, weakness, lethargy, liver damage, skin lesions, and muscle and fat lost. It was observed that optical and electronic properties of assembled nanoparticles more enhanced than that of monodisperse nanoparticles for SERS applications. Therefore gold nanosphere agglomerates were utilized in the determination of $1.0x10^{-6}$ M cysteine via colorimetric and SERS methods. As far as we know the quantitative SERS detection of cysteine at this low concentration and the usage of the nanoparticle network for the quantitative SERS determination of the linker molecule have not been explored yet. The results have shown the possibility of cysteine detection in biological samples by using the proposed SERS method. Detection of selenocysteine which is known as 21th amino acid is under investigation.

REFERENCES

Abid, J. P., Abid, M., Bauer, C., Girault, H. H., & Brevet, P. F. (2007). Controlled Reversible Adsorption of Core-Shell Metallic Nanoparticles at the Polarized water/1,2-Dichloroethane Interface Investigated by Optical Second-Harmonic Generation. *J. Phys. Chem. C. , 111*, 8849-8855.

Alivisatos, A. P. (1996). Perspectives on the Physical Chemistry of Semiconductor Nanocrystals. *J. Phys. Chem. , 100* (31), 13226-13239.

Aryal, S., Remant, B., Dharmaraj, N., Bhattarai, N., Kim, C. H., & Kim, H. Y. (2006). Spectroscopic identification of S-Au interaction in cysteine capped gold nanoparticles. *Spectrochimica Acta Part A. , 63*, 160–163.

Baueer, L. A., Birenbaum, N. S., & Meyer, G. J. (2004). Biological applications of high aspect ratio nanoparticles. *J . Ma t e r . C h em. , 14*, 517-526.

Bisht, S., Feldmann, G., Soni, S., Ravi, R., Karikar, C., Maitra, A., et al. (2007). Polymeric nanoparticle-encapsulated curcumin ("nanocurcumin"):a novel strategy for human cancer therapy. *Journal of Nanobiotechnology , 5* (3).

Bouhelier, A., Beversluis, M., & Novotny, L. (2003). Characterization of nanoplasmonic structures by locally excited photoluminescence. *Appl. Phys. Lett. , 83*, 5041 –5043.

Bouhelier, A., Beversluis, M., & Novotny, L. (2003). Plasmon-coupled tip-enhanced near-field optical microscopy. *J. Microsc. , 210* (3), 220-224.

Busbee, B., Obare, S., & Murphy, C. J. (2003). An Improved Synthesis of High-Aspect-Ratio Gold Nanorods. *Advanced Materials , 15*, 414-416.

Cang, H., Sun, T., Li, Z. Y., Chen, J. Y., Wiley, B. J., Xia, Y. N., et al. (2005). Gold nanocages as contrast agents for spectroscopic optical coherence tomography. *Opt. Lett. , 30* , 3048–3050.

Caswell, K. K., Wilson, J. N., Bunz, U. H., & Murphy, C. J. (2003). Preferential End-to-End Assembly of Gold Nanorods by Biotin−Streptavidin Connectors. *J. Am. Chem. Soc. , 125* (46), 13914-13915.

Chang, J. Y., Wu, H., Chen, H., Ling, Y. C., & Tan, W. (2005). Oriented assembly of Au nanorods using biorecognition system. *Chem. Commun.* , 1092-1094.

Chang, S. S., Shih, C. W., Chen, C. D., Lai, W. C., & Chris Wang, C. (1999). The Shape Transition of Gold Nanorods. *Langmuir , 15*, 701-709.

Chen, C. C., Lin, Y. P., Wang, C. W., Tzeng, H. C., Wu, C. H., Chen, Y. C., et al. (2006). DNA-gold nanorod conjugates for remote control of localized gene expression by near infrared irradiation. *J. Am. Chem. Soc. , 128*, 3709–3715.

Chen, J., Sorensen, C., Klabunde, K., & Hadjipanayis, G. (1995). Enhanced magnetization of nanoscale colloidal cobalt particles. *Physical Review B , 51* (17).

Chon, W. M., Bullen, C., Zijlstra, P., & Gu, M. (2007). Spectral encoding on Gold Nanorods Doped in a Silica Sol–Gel Matrix and Its Application to High-Density Optical Data Storage. *Adv. Funct. Mater. , 17*, 875-880.

Cullum, B. M., & Vo-Dinh, T. (2001). Nanosensors for biochemical analysis of single cells. *Chimica Oggi. , 19*, 58–62.

Eghtedari, M., Oraevsky, A., Copland, J. A., Kotov, N. A., Conjusteau, A., & Motamedi, M. (2007). High sensitivity of in vivo detection of gold nanorods using a laser optoacoustic imaging system. *Nano Lett. , 7*, 1914–1918.

Esumi, K., Matsuhisa, K., & Torigoe, K. (1995). Preparation of rodlike gold particles by UV irradiation using cationic micelles as a template. *Langmuir , 11* (9), 3285-3287.

Eustis, E., & El Sayed, M. (2006). Why gold nanoparticles are more precious than pretty gold: Noble metal surface plasmon resonance and its enhancement of the radiative and nonradiative properties of nanocrystals of different shapes. *Chem. Soc. Rev. , 35*, 209-217.

Eychmüller, A. (2000). Structure and Photophysics of Semiconductor Nanocrystals. *J. Phys. Chem. B , 104* (28), 6514-6528.

Foley, S., & Enescu, M. (2007). A Raman spectroscopy and theoretical study of zinc–cysteine complexation. *Vibrational Spectroscopy , 44*, 256-265.

Foss, C. A., Hornyak, G. L., Stockert, J. A., & Martin, C. R. (1992). Optical Properties of Composite Membranes Containing Arrays of Nanoscopic Gold Cylinders. *J. Phys. Chem. , 96*, 1491-1499.

Foss, C. A., Hornyak, G. L., Stockert, J. A., & Martin, C. R. (1994). Template-Synthesized Nanoscopic Gold Particles: Optical Spectra and the Effects of Particle Size and Shape. *J. Phys. Chem. , 98* (11), 2963–2971.

Frens, G. (1973). Controlled nucleation for the regulation of the particle size in monodisperse gold solutions. *Nat. Phys. Sci. , 241*, 20-24.

Fu, H. B., & Yao, J. N. (2001). Size Effects on the Optical Properties of Organic Nanoparticles. *J. Am. Chem. Soc. , 123* (7), 1434-1439.

Gao, J., Bender, C. M., & Murphy, C. J. (2003). Dependence of the Gold Nanorod Aspect Ratio on the Nature of the Directing Surfactant in Aqueous Solution. *Langmuir , 19*, 9065-9070.

Gole, A., & Murphy, C. J. (2004). Seed-Mediated Synthesis of Gold Nanorods: Role of the Size and Nature of the Seed. *Chem. Mater. , 16*, 3633-3640.

Gou, L., & Murphy, C. J. (2005). Fine-Tuning the Shape of Gold Nanorods. *Chem. Mater. , 17*, 3668-3672.

Haes, A. J., Zou, S., Schatz, G. C., & Van Duyne, R. P. (2004). Nanoscale Optical Biosensor: Short Range Distance Dependence of the Localized Surface Plasmon Resonance of Noble Metal Nanoparticles. *J. Phys. Chem. B , 108* (22), 6961-6968.

Harris, P. J. (1999). *Carbon nanotubes and related nanostructures.* Cambridge: Cambridge university press.

Hazarika, P., Ceyhan, B., & Niemeyer, C. M. (2004). Reversible Switching of DNA–Gold Nanoparticle Aggregation. *Angewandte Chemie , 116*, 6631–6633.

Hu, X., Cheng, W., Wang, T., Wang, E., & Dong, S. (2005). Well-ordered end-to-end linkage of gold nanorods. *Nanotechnology , 16* (10), 2164-2169.

Huang, X., Neretina, S., & El Sayed, M. (2009). Gold Nanorods: From Synthesis and Properties to Biological and Biomedical Applications. *Adv. Mater. , 21*, 4880–4910.

Huff, T. B., Hansen, M. N., Zhao, Y., Cheng, J. X., & Wei, A. (2007). Controlling the cellular uptake of gold nanorods. *Langmuir , 23*, 1596–1599.

Jana, N. R. (2005). Gram-Scale Synthesis of Soluble, Near-Monodisperse Gold Nanorods and Other Anisotropic Nanoparticles. *Small , 1*, 875-882.

Jana, N. R., Gearheart, L., & Murphy, C. J. (2001). Evidence for Seed-Mediated Nucleation in the Chemical Reduction of Gold Salts to Gold Nanoparticles. *Chem. Mater. , 13* (7), 2313-2322.

Jana, N. R., Gearheart, L., & Murphy, C. J. (2001). Seed-Mediated Growth Approach for Shape-Controlled Synthesis of Spheroidal and Rod-like Gold Nanoparticles Using a Surfactant Template. *Advanced Materials , 13* (18), 1389-1393.

Jana, N. R., Gearheart, L., & Murphy, C. J. (2001). Wet Chemical Synthesis of High Aspect Ratio Cylindrical Gold Nanorods. *J. Phys. Chem. B , 105* (19), 4065-4067.

Jana, N. R., Gearheart, L., & Murphy, C. J. (2001). Wet chemical synthesis of silver nanorods and nanowiresof controllable aspect ratio. *Chem. Commun. ,* 617-618.

Javier, D. J., Nitin, N., Roblyer, D. M., & Richards, K. R. (2008). Metal-based nanorods as molecule-specific contrast agents for reflectance imaging in 3D tissues. *J. Nanophoton. , 2* (023506).

Jiang, X. C., & Pileni, M. P. (2007). Gold nanorods: Influence of various parameters as seeds,solvent, surfactant on shape control. *Colloids and Surfaces A: Physicochem. Eng. Aspects. , 295*, 228-232.

Jing, C., & Fang, Y. (2006). Experimental (SERS) and theoretical (DFT) studies on the adsorption behaviors of L-cysteine on gold/silver nanoparticles. *Chemical Physics ,* 27-31.

Johnson, C. J., Dujardin, E., Davis, S. A., Murphy, C. J., & Mann, S. (2002). Growth and form of gold nanorods prepared by seed-mediated,surfactant-directed synthesis. *J. Mater. Chem. , 12*, 1765-1770.

Khlebtsov, B. N., Khanadeev, V. A., Bogatyrev, V. A., Dykman, L. A., & Khlebtsov, N. G. (2009). Fabrication, Stabilization, and Optical Properties of Gold Nanorods with Silver Shells. *Nanotechnologies In Russia. , 4*, 453-466.

Kim, F., Song, J. H., & Yang, P. (2002). Photochemical Synthesis of Gold Nanorods. *J. Am. Chem. Soc. , 124*, 14316-14317.

Lee, G. J., Shin, S. I., Kim, Y. C., & Oh, S. G. (2004). Preparation of silver nanorods through the control of temperature and pH of reaction medium. *Materials Chemistry and Physics , 84*, 197-204.

Lee, P. C., & Meisel, D. (1982). Adsorption and surface-enhanced Raman of dyes on silver and gold sols. *J. Phys. Chem. , 86* (17), 3391-3395.

Li, C., Wu, C., Zheng, J., Lai, J., Zhang, C., & and Zhao, Y. (2010). LSPR Sensing of Molecular Biothiols Based on Noncoupled Gold Nanorods. *Langmuir , 26*, 9130-9135.

Li, Z. P., Duan, X. R., Liu, C. H., & Du, B. A. (2006). Selective determination of cysteine by resonance light scattering technique based on self-assembly of gold nanoparticles. *Analytical Biochemistry , 351*, 18-25.

Liao, H., & Hafner, J. (2005). Gold nanorod bioconjugates. *Chem. Mater. , 17*, 4636–4641.

Liu, F. K., Chang, Y. C., Ko, F. H., & Chu, T. C. (2004). Microwave rapid heating for the synthesis of gold nanorods. *Materials Letters. , 58*, 373–377.

Liu, M. Z., & Guyot-Sionnest, P. (2005). Mechanism of Silver(I)-Assisted Growth of Gold Nanorods and Bipyramids. *J. Phys. Chem. B , 109* (47), 22192-22200.

Liu, M., & Guyot Sionnest, P. (2004). Synthesis and Optical Characterization of Au/Ag Core/Shell Nanorods. *J. Phys. Chem. B. , 108*, 5882-5888.

Lofton, C., & Sigmund, W. (2005). Mechanisms Controlling Crystal Habits of Gold and Silver Colloids. *Adv. Funct. Mater. , 15* (7), 1197–1208.

Loo, C., Lowery, A., Halas, N., West, J., & Drezek, R. (2005). Immunotargeted nanoshells for integrated cancer imaging and therapy. *Nano Lett. , 5*, 709–711.

Martin, B. R., Dermody, D. J., Reiss, B. D., Fang, M. M., Lyon, L. A., Natan, M. J., et al. (1999). Orthogonal Self-Assembly on Colloidal Gold-Platinum Nanorods. *Advanced Materials , 11* (12), 1021-1025.

Millstone, J. E. (2008). Iodide Ions Control Seed-Mediated Growth of Anisotropic Gold Nanoparticles. *Nano Lett. , 8*, 2526-2529.

Miranda, O. R., Dollahon, N. R., & Ahmadi, T. S. (2006). Critical Concentrations and Role of Ascorbic Acid (Vitamin C) in the Crystallization of Gold Nanorods within Hexadecyltrimethyl Ammonium Bromide (CTAB)/Tetraoctyl Ammonium Bromide (TOAB) Micelles. *Crystal Growth & Design. , 6*, 2747-2753.

Mougin, K., Darwich, S., Vidal, L., & H., H. (2010). Combined Electrostatic-Covalent Building of Au NPs Multilayers and Their Size-Enhanced Cohesive and SERS Properties. *Advances in Physical Chemistry* .

Murphy, C. J. (2005). Anisotropic Metal Nanoparticles: Synthesis, Assembly, and Optical Applications. *J. Phys. Chem. B. , 109*, 13857-13870.

Murphy, C. J., & Jana, N. R. (2002). Controlling the Aspect Ratio of Inorganic Nanorods and Nanowires. *Adv. Mater. , 14* (1).

Murphy, C. J., Sau, T. K., Gole, A., & Orendorff, C. J. (2005). Surfactant-Directed Synthesis and Optical Properties of One-Dimensional Plasmonic Metallic Nanostructures. *MRS BULLETIN* .

Nagarajan, R. A. (2008). Nanoparticles: Building Blocks for Nanotechnology. *ACS Symposium Series.* Washington, DC: American Chemical Society.

Nanoparticles and their Applications. (2007). Retrieved 01 24, 2011, from understandingnano.com: http://www.understandingnano.com/nanoparticles.html

Nehl, C. L., Liao, H. W., & Hafner, J. H. (2006). Optical properties of star-shaped gold nanoparticles. *Nano Lett. , 6*, 683–688.

Nie, S., & Emory, S. R. (1997). Probing Single Molecules and Single Nanoparticles by Surface-Enhanced Raman Scattering. *Science , 275* (5303), 1102-1106.

Nie, Z., Fava, D., Kumacheva, E., Zou, S., Walker, G. C., & Rubinstein, M. (2007). Self-assembly of metal–polymer analogues of amphiphilic triblock copolymers. *Nature Materials , 6*, 609-614.

Nikoobakht, B., & El Sayed, M. A. (2001). Evidence for Bilayer Assembly of Cationic Surfactants on the Surface of Gold Nanorods. *Langmuir. , 17*, 6368-6374.

Nikoobakht, B., & El-Sayed, M. A. (2003). Preparation and Growth Mechanism of Gold Nanorods (NRs) Using Seed-Mediated Growth Method. *Chem. Mater. , 15*, 1957-1962.

Noguez, C. (2007). Surface Plasmons on Metal Nanoparticles: The Influence of Shape and Physical Environment. *J. Phys. Chem. C , 111* (10), 3806-3819.

Olson, R. Y., Schwartzberg, A. M., Orme, C. A., Talley, C. E., O'Connell, B., & Zhang, J. Z. (2008). Hollow Gold−Silver Double-Shell Nanospheres: Structure, Optical Absorption, and Surface-Enhanced Raman Scattering. *J. Phys. Chem. C , 112* (16), 9319-6329.

Olson, Y., Schwartzberg, M. A., Orme, C. A., Talley, C., O'Connell, B., & Zhang, Z. (2008). *J. Phys. Chem. C.* , 6319-6329.

Ozin, G. A., & Arsenault, A. C. (2009). *Nanochemistry; A Chemical Approach to Nanomaterials.* RCS Publishing.

Park, S., Lim, J. H., Chung, S. W., & Mirkin, C. A. (2004). Self-Assembly of Mesoscopic Metal-Polymer Amphiphiles. *Science , 303* (5656), 348-351.

Perez-Juste, J., Pastoriza-Santos, I., Liz-Marzan, L. M., & Mulvaney, P. (2005). Gold nanorods: Synthesis, characterization and applications. *Coordination Chemistry Reviews. , 249*, 1870-1901.

Placido, T., Comparelli, R., Giannici, F., Cozzoli, P. D., Capitani, G., Striccoli, M., et al. (2009). Photochemical Synthesis of Water-Soluble Gold Nanorods: The Role of Silver in Assisting Anisotropic Growth. *Chem. Mater. , 21*, 4192-4202.

Pyatenko, A., Yamaguchi, M., & Suzuki, M. (2007). Synthesis of Spherical Silver Nanoparticles with Controllable Sizes in Aqueous Solutions. *J. Phys. Chem. C , 111*, 7910-7917.

Raman Spectroscopy. (no date). Retrieved 01 27, 2011, from Horiba Scientific: http://www.horiba.com/scientific/products/raman-spectroscopy/tutorial-faqs/raman-tutorial/raman-spectroscopy/

Rayavarapu, R. G. (2010). Iodide Impurities in Hexadecyltrimethylammonium Bromide (CTAB) Products: Lot-Lot Variations and Influence on Gold Nanorod Synthesis. *Langmuir , 26*, 5050–5055.

Rostro-Kohanloo, B. C., Bickford, L. R., Payne, C. M., Day, E. S., Anderson, L. E., Zhomg, M., et al. (2009). The stabilization and targeting of surfactant-synthesized gold nanorods. *Nanotechnology , 20* (434005).

Rozhkova, E., Ulasov, I., Lai, B., Dimitrijevic, N., Lesniak, M., & Rajh, T. (2009). A High-Performance Nanobio Photocatalyst for Targeted Brain Cancer Therapy. *Nano Letters , 9* (9), 3337–3342.

Rusin, O., Luce, N. N., & Agbaria, R. A. (2004). Visual Detection of Cysteine and Homocysteine. *J. Am. Chem. S. , 126*, 438-439.

Rusin, O., Luce, N. N., Agbaria, R. A., Escobedo, J. O., Jiang, S., Warner, I. M., et al. (2004). Visual Detection of Cysteine and Homocysteine. *J. Am. Chem. Soc. , 126*, 438-439.

Chang, S. S.,Shih, C. W., Chen, C. D., Lai, W. C., & Wang, C. R. (1999). The Shape Transition of Gold Nanorods. *Langmuir , 15*, 701-709.

Salem, A. K., Searson, P. C., & Leong, K. W. (2003). Multifunctional nanorods for gene delivery. *Nature Mater. , 2*, 668-671.

Sau, T. K. (2004). Seeded High Yield Synthesis of Short Au Nanorods in Aqueous Solution. *Langmuir , 20*, 6414-6420.

Schmid, G. (1992). Large clusters and colloids. Metals in the embryonic state. *Chem. Rev. , 92* (8), 1709-1727.

Schultz, D. A. (2003). Plasmon Resonant Particles for Biological Detection. *Curr. Opin. Biotechnol. , 14*, 13-22.

Sharma, J., Chhabra, R., Liu, Y., Ke, Y., & Yan, H. (2006). DNA-Templated Self-Assembly of Two-Dimensional and Periodical Gold Nanoparticle Arrays. *Angewandte Chemie International Edition , 45*, 730-735.

Sigma Aldrich Co. (2011, 09 27). *L-Cysteine.* Retrieved 09 28, 2011, from www.sigmaaldrich.com: http://www.sigmaaldrich.com/catalog/ProductDetail.do?lang=en&N4=W326305|ALDRICH&N5=SEARCH_CONCAT_PNO|BRAND_KEY&F=SPEC

Skrabalak, S. E., Chen, J., Au, L., Lu, X., Li, X., & Xia, Y. (2007). Gold nanocages for biomedical applications. *Adv. Mater. , 19*, 3177–3184.

Smith, D. K. (2009). Iodide in CTAB Prevents Gold Nanorod Formation. *Langmuir. , 25*, 9518–9524.

Sohn, K., Kim, F., Pradel, K. C., Wu, J., Peng, Y., Zhou, F., et al. (2009). Construction of Evolutionary Tree for Morphological Engineering of Nanoparticles. *Acs. Nano. , 3*, 2191-2198.

Sokolov, K., Follen, M., Aaron, J., Pavlova, I., & Malpica, A. (2003). Real-time vital optical imaging of precancer using anti-epidermal growth factor receptor antibodies conjugated to gold nanoparticles. *Cancer Res. , 63*, 1999–2004.

Sudeep, P. K., Joseph, S. T., & Thomas, K. G. (2005). Selective Detection of Cysteine and Glutathione Using Gold Nanorods. *J. Am. Chem. Soc. , 127* (18), 6516-6517.

Sue, K., Suzuki, M., Arai, K., Ohashi, T., Ura, H., Matsui, K., et al. (2006). Size-controlled synthesis of metal oxide nanoparticles with a flow-through supercritical water method. *Green Chem. , 8* (7), 634-638.

Sun, Z., Ni, W., Yang, Z., Kou, X., Li, L., & Wang, J. (2008). pH-Controlled Reversible Assembly and Disassembly of Gold Nanorods. *Small , 4*, 1287–1292.

Tan, Y., Li, Y., & Zhu, D. (2003). Preparation of silver nanocrystals in the presence of aniline. *Journal of Colloid and Interface Science , 258*, 244-251.

Thomas, K. G., Barazzouk, S., Ipe, B. I., Joseph, S. T., & Kamat, P. V. (2004). Uniaxial Plasmon Coupling through Longitudinal Self-Assembly of Gold Nanorods. *J. Phys. Chem. B , 108* (35), 13066-13068.

Turkevich, J., C., S. P., & Hillier, J. (1951). A study of the nucleation and growth processes in the synthesis of colloidal gold. *Discuss. Faraday Soc. , 11*, 55-75.

Uechi, I. A. (2008). Photochemical And Analytical Applications Of Gold Nanoparticles And Nanorods Utilizing Surface Plasmon Resonance. *Anal. Bioanal. Chem. , 391*, 2411-2421.

van der Zande, B. M., Bohmer, M. R., Fokkink, L. G., & Schonenberger, C. (2000). Colloidal Dispersions of Gold Rods: Synthesis and Optical Properties. *Langmuir , 16* (2), 451-458.

van der Zande, B. M., Böhmer, M. R., Fokkink, L. G., & Schönenberger, C. (1997). Aqueous Gold Sols of Rod-Shaped Particles. *J. Phys. Chem. B , 101* (6), 852-854.

Varghese, N., Vivekchand, S. R., Govindaraj, A., & Rao, C. N. (2008). A calorimetric investigation of the assembly of gold nanorods to form necklaces. *Chemical Physics Letters , 450*, 340-344.

Wang, H., Huff, T. B., ZweifelD, A., He, W., Low, P. S., Wei, A., et al. (2005). In vitro and in vivo two-photon luminescence imaging of single gold nanorods. *Proc. Natl. Acad. Sci. USA , 102*, 15752–15756.

Wang, Z. L., Mohamed, M. B., Link, S., & El-Sayed, M. A. (1999). Crystallographic facets and shapes of gold nanorods of different aspect ratios. *Surf. Sci. , 440*, L809-L814.

Wikimedia Foundation, Inc. (2011, 09 16). *Ascorbic acid.* Retrieved 09 16, 2011, from Wikipedia: http://en.wikipedia.org/wiki/Ascorbic_acid

Wiley, B. J., Chen, Y., McLellan, J. M., Xiong, Y., Li, Z. Y., Ginger, D., et al. (2007). Synthesis and Optical Properties of Silver Nanobars and Nanorice. *Nano Letters , 7* (4), 1032-1036.

Wu, H. Y., Huang, W. L., & Huang, M. H. (2007). Direct High-Yield Synthesis of High Aspect Ratio Gold Nanorods. *Cryst. Growth Des. , 7*, 831-835.

Wu, W., He, Q., & Jiang, C. (2008). Magnetic Iron Oxide Nanoparticles: Synthesis and Surface Functionalization Strategies. *Nanoscale Research Letter , 3* (11), 397–415.

Xia, Y., & Halas, N. J. (2005). Shape-controlled Synthesis and Surface Plasmonic Properties of Metallic Nanostructures. *MRS Bulletin , 30*.

Xiang, Y., Wu, X., Liu, D., Li, Z., Chu, W., Feng, L., et al. (2008). Gold Nanorod-Seeded Growth of Silver Nanostructures: From Homogeneous Coating to Anisotropic Coating. *Langmuir , 24*, 3465-3470.

Yang, D. P., & Cui, D. X. (2008). Advances and Prospects of Gold Nanorods. *Chem. Asian J. , 3*, 2010 – 2022.

Yang, Y., Matsubara, S., Xiong, L., Hayakawa, T., & Nogami, M. (2007). Solvothermal Synthesis of Multiple Shapes of Silver Nanoparticles and Their SERS Properties. *J. Phys. Chem.C , 111*, 9095-9104.

Ying, Y., Chang, S. S., Lee, C. L., & Wang, C. (1997). Gold Nanorods: Electrochemical Synthesis and Optical Properties. *J. Phys. Chem. B , 101* (34), 6661–6664.

Yu, C. X., Nakshatri, H., & Irudayaraj, J. (2007). Identity profiling of cell surface markers by multiplex gold nanorod probes. *Nano Lett. , 7*, 2300–2306.

Yu, Y. Y., Chang, S. S., Lee, C. L., & Wang, C. R. (1997). Gold Nanorods: Electrochemical Synthesis and Optical Properties. *J. Phys. Chem. B , 101* (34), 6661-6664.

Zhang, F. X., Han, L., Israel, L. B., Daras, J. G., Mayr, M. M., Ly, N. K., et al. (2002). Colorimetric detection of thiol-containing amino acids using gold nanoparticles. *Analyst , 127*, 462-465.

Zhang, S., Kou, X., Yang, Z., Shi, Q., Stucky, G. D., Sun, L., et al. (2007). Nanonecklaces assembled from gold rods, spheres, and bipyramids. *Chem. Commun.* , 1816-1818.

Zhou, Q., Chao, Y., Li, Y., Xu, W., Wu, Y., & Zheng, J. (2007). Contribution of Charge-Transfer Mechanisms to Surface-Enhanced Raman Scattering with Near-IR Excitation. *Chem PhysChem , 8* (6), 921 – 925.